Qubit Recycling Revisited

Extended Version

HANRU JIANG, Beijing Institute of Mathematical Sciences and Applications, China

Reducing the width of quantum circuits is crucial due to limited number of qubits in quantum devices. This paper revisit an optimization strategy known as *qubit recycling* (alternatively *wire-recycling* or *measurement-and-reset*), which leverages gate commutativity to reuse discarded qubits, thereby reducing circuit width. We introduce *qubit dependency graphs* (QDGs) as a key abstraction for this optimization. With QDG, we isolate the computationally demanding components, and observe that qubit recycling is essentially a matrix triangularization problem. Based on QDG and this observation, we study qubit recycling with a focus on complexity, algorithmic, and verification aspects. Firstly, we establish qubit recycling's NP-hardness through reduction from Wilf's question, another matrix triangularization problem. Secondly, we propose a QDG-guided solver featuring multiple heuristic options for effective qubit recycling. Benchmark tests conducted on RevLib illustrate our solver's superior or comparable performance to existing alternatives. Notably, it achieves optimal solutions for the majority of circuits. Finally, we develop a certified qubit recycler that integrates verification and validation techniques, with its correctness proof mechanized in Coq.

CCS Concepts: • **Hardware → Quantum computation**; **Circuit optimization**; • **Software and its engineering → Software verification**.

Additional Key Words and Phrases: Quantum Circuit Optimization, Complexity, Certified Compilation

1 INTRODUCTION

Reducing the cost of a quantum circuit is crucial, particularly for near-term quantum computers with limited computational resources [Preskill 2018]. One commonly used metric for assessing cost is the circuit *width*, which corresponds to the number of qubits used in a quantum circuit. In fault-tolerant quantum computing, where the overhead of a logical qubit using quantum error-correction is substantial [Fowler et al. 2012], circuit width becomes particularly important.

Among the various approaches to minimizing circuit width, qubit recycling, also known as wire recycling or reclaiming qubit via measurement-and-reset, has been found to be effective and intuitive. Analytic analysis [DeCross et al. 2023] on well-structured circuit families showcased its capacity to significantly reduce circuit width, sometimes exponentially or to a constant size. Empirical evaluation [DeCross et al. 2023; Hua et al. 2023; Paler et al. 2016] further indicated that qubit recycling can achieve reductions in circuit width up to 80–90%. Moreover, recent research [Hua et al. 2023] illustrated that leveraging mid-circuit measurement for qubit recycling might enhance fidelity in specific circuits executed on real quantum hardware.

The idea behind qubit recycling is that once a qubit is measured and discarded, it becomes disentangled from the other qubits and can be reused as a fresh qubit by resetting it. Qubit recycling further leverages the commutativity of local quantum operations to create more opportunities for qubit reuse, allowing for earlier measurements or deferring allocation.

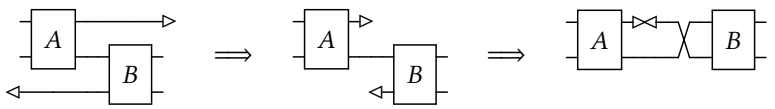

Author's address: Hanru Jiang, Beijing Institute of Mathematical Sciences and Applications, Beijing, China, hanru@bimsa.cn.

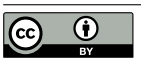

The above is an example illustrating a qubit recycling procedure, which rewrites the left most circuit into the right most one. In each circuit, a horizontal line represents a qubit, a box represents a quantum gate applied to the qubits it covers, and the gates are applied from left to right. Starting from the left-most circuit, we first postpone the allocation (denoted by $\triangleleft$) and bring forward the measurement (denoted by $\triangleright$). When the measurement is earlier than the allocation, we reuse the top qubit as the bottom one. As a result, the circuit width is reduced by one.

Despite its efficacy, qubit recycling remains an underexplored topic with several fundamental questions yet to be answered, including:

(1) *What is the computational complexity of minimizing circuit width using qubit recycling?* Previous works [DeCross et al. 2023; Hua et al. 2023; Paler et al. 2016] develop (exponential-time) exact or heuristic-based algorithms for qubit recycling. However, the intrinsic difficulty of this problem remains unclear.
(2) *How can we ensure the correctness of a qubit recycler?* Existing approaches on verified compilation for quantum programs [Hietala et al. 2021; Tao et al. 2022] do not directly apply to qubit recycling. These approaches primarily concentrate on rewriting-based optimizations that *preserve* circuit width, while qubit recycling aims to *reduce* circuit width.

To better understand qubit recycling and address these questions, it is essential to have a problem abstraction that isolates the computationally intensive part from simpler circuit rewritings based on gate commutativity. With this in mind, we revisit qubit recycling and address the aforementioned questions. The contribution includes:

- We identify computational dependencies between *qubits* as the key factor in qubit recycling and formalize these dependencies using *qubit dependency graphs* (QDGs). A QDG concisely captures the necessary information to determine valid qubit *recycling strategies*, specifying which qubit can be reused by another. With the matrix representation of QDGs, we observe that qubit recycling is essentially a matrix triangularization problem. This observation proves valuable in studying complexity, algorithm design, and verification of qubit recyclers.
- We prove that qubit recycling is NP-hard. The proof is based on a reduction from Wilf's question, another triangularization problem which is known to be NP-complete.
- Based on the structure of the triangularization problem, we develop an efficient solver featuring multiple heuristics. To evaluate the optimality of the solutions, we employ SCIP [Bolusani et al. 2024] to solve the original problem, or provide an estimated upper-bound on the size of optimal solutions in case where finding optimal solutions is not feasible. Evaluation on the RevLib [Wille et al. 2008] benchmark shows that our solver consistently yields equally good or superior solutions when compared to existing methods, and achieves optimal solutions for the majority of the circuits.
- We formalize a weaker correctness criterion for quantum circuit optimizations, allowing for qubit renaming and reuse. To support dynamic qubit allocation and discard, our semantics decouple qubit identity from their physical location by explicitly incorporating I/O qubits in the circuit. Our correctness formulation is transitive and congruent to sequential composition, facilitating modular verification of optimization passes.
- We propose a certified qubit recycler design that integrates compiler verification and validation techniques. This recycler comprises an untrusted solver handling the computationally intensive task of finding recycling strategies, and a verified circuit rewriter which also validates the recycling strategy. The validation process aligns with part of the circuit transformations, namely topological sorting. This is the point where we integrate verification and validation in a single module. This approach avoids the need to individually verify the solver, and ensures our proof is resilient to potential future updates to the solver.

- We implement the certified qubit recycler in Coq. Byproducts of the Coq development include a verified Kahn's algorithm for topological sorting, and a version of the coherence theorem for symmetric monoidal categories.

This work focuses on qubit reuse independent of considerations of the architecture of a quantum computer. In addition, this work focuses solely on qubit reuse through topological deformation, without considering other non-trivial semantic-based circuit rewritings such as CNOT cancellations.

Outline. Sec. 2 overviews the main results. Sec.3 presents the necessary language and problem settings. Subsequently, Sec.4 formalizes QDGs, and Sec.5 proves the NP-hardness of qubit recycling. We then proceed to develop the certified qubit recycler in Sec.6. Finally, we present and evaluate our algorithms and ILP model for qubit recycling in Sec. 7, and discuss related work in Sec.8.

2 INFORMAL DEVELOPMENT

In this section, we first briefly overview qubit recycling (Sec.2.1), then outline the challenges associated with addressing the questions raised in Sec.1 and present our approaches to tackle them (Sec.2.2). Throughout this section, we use Fig.1 as a running example.

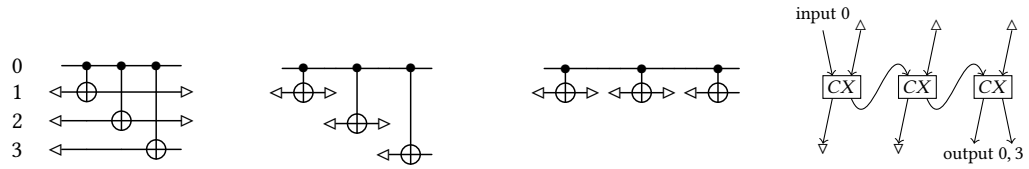

(a) Input circuit. (b) Topological deformation. (c) Renaming and reusing. (d) DAG repr. of Fig. 1a.

Fig. 1. A running example of qubit recycling.

2.1 Background: Quantum Circuits and the Qubit Recycling Problem

Quantum circuits. Quantum programs are commonly represented using quantum circuits, which describe a sequence of quantum operations or gates. For instance, Fig.1a is a 4-qubit quantum circuit. Each horizontal line in the circuit corresponds to a qubit, numbered as 0, 1, 2, and 3. Quantum gates are applied from left to right. A $\triangleleft$ symbol represents the allocation of the qubit, while a $\triangleright$ symbol represents a discard gate. The discard gate effectively measures the qubit and discards the measurement result. A qubit used without allocation (e.g, qubit 0) is considered an *input qubit*, while a qubit lacking a discard gate (e.g. qubit 0 and 3) is referred to as *output qubit*. Input and output qubits may differ. For unitary gates, we consider only arbitrary 2-qubit gates for now. The gate used in Fig.1, is the *CX* gate, which is an arbitrary and irrelevant choice. It may help understanding if we temporarily forget the semantics of *CX*. In Fig.1, the *CX* gate is denoted by a vertical line connecting $\bullet$ and $\oplus$, indicating the two qubits it operates on. The vertical line has no effect on a qubit if the crossing is not annotated with $\bullet$ or $\oplus$.

Semantic preserving circuit transformations. In this section, we do not delve into the semantics of a circuit but instead introduce two transformations that preserve semantics.

- *Topological deformation* (Fig. 2a) states that two gates commute if they are applied on disjoint sets of qubits. Two circuits are considered *topologically identical* if they are identical modulo topological deformations.
- *Qubit reusing* (Fig. 2b) states that if the discard of a qubit precedes the allocation of another qubit, the former can be reused as the latter. We use the symbol $\approx$ instead of $=$ to indicate

(a) Topological deformation.
Here ⊣ means one or more qubits.

(b) Qubit reusing

Fig. 2. Semantic preserving circuit transformations.

that these circuits are not identical but observably equivalent modulo renaming of I/O qubits. Qubit reusing leads to a reduction in circuit width by 1.

Qubit recycling. Given a quantum circuit, qubit recycling aims to *find a topologically identical circuit that maximizes qubit reusing*, effectively minimizing the circuit width. Consider the circuit in Fig.1a. One can first reshape the circuit using topological deformation and obtain Fig.1b. Then, by renaming qubit 3 into 2 and qubit 2 into 1, we obtain Fig.1c with width reduced by 2.

2.2 Challenges and Our Approach

Our goal is to solve the qubit recycling problem correctly and efficiently. Specifically, we aim to understand the problem's complexity, develop a solution that runs in a reasonable time, and create a certified optimizer for qubit recycling. In the following, we outline the challenges we face and present our approaches to achieving these goals.

2.2.1 The Search Space is Too Large to Analyze. Given a circuit, the set of its topologically identical circuits becomes unmanageably large as the number of gates increases. This set comprises all the topological orderings of the circuit's directed acyclic graph (DAG) representation. Merely computing the size of this set is #P-complete [Brightwell and Winkler 1991].

For instance, the DAG representation of the circuit Fig. 1a is shown in Fig. 1d. The number of all its topological orderings is more than 100, which is significantly larger than 4, the qubit count.

Our approach: decomposition using recycling strategies. Our first observation is that by employing *recycling strategies*, we can decompose the qubit recycling problem and avoid directly analyzing the set of topologically identical circuits. A recycling strategy is an injective partial map on qubits, where each pair $q \hookrightarrow q'$ in the map denotes that q' reuses q. Every solution to the qubit recycling problem corresponds to a recycling strategy $\hookrightarrow$, and its size $|\hookrightarrow|$ represents the number of reused qubits. Conversely, given a *valid* $\hookrightarrow$, we can efficiently construct a solution of the same width.

Therefore, to find an optimal solution for qubit recycling, it suffices to:

(i) Find a largest *valid* recycling strategy $\hookrightarrow$ for the input circuit
(ii) Construct a solution using $\hookrightarrow$ and the input circuit.

Sub-problem (ii) can be solved in linear time, which is essentially topological sorting. Regarding sub-problem (i), it is evident that the number of all recycling strategies (valid or invalid) is only relevant to the circuit's width. In practice, the search space for sub-problem (i) is much smaller than that for the original qubit recycling problem.

In our example circuit, since there are only 2 discarded qubits and 3 allocated qubits, there are at most 12 recycling strategies of interest, and only 4 of them are valid: $\{1 \hookrightarrow 2\}$, $\{2 \hookrightarrow 3\}$, $\{1 \hookrightarrow 3\}$, and $\{1 \hookrightarrow 2, 2 \hookrightarrow 3\}$. With the largest strategy, a solution for qubit recycling is obtained by connecting discard of qubit 1 and 2 with allocation of qubit 2 and 3, respectively, then perform a topological sort on it.

2.2.2 Gap 1: What is a Valid Recycling Strategy? A straightforward answer is a recycling strategy corresponding to a solution of the original problem, but this requires finding a solution in the first place. Intuitively, there should be a simpler way: a recycling strategy is essentially a relation over qubits, it should be possible to check its validity knowing only qubit relationships.

Our approach: We introduce *qubit dependency graphs* (QDGs) as the key abstraction for analyzing recycling strategies and verifying their validity. The QDG of a circuit C, denoted as $QDG(C)$, is a directed graph whose vertices represent the qubits in C. An edge $q \to q'$ in $QDG(C)$ indicates a computational dependency, it means that some computations involving q must occur before those involving q'. Concretely, $q \to q'$ if either (i) there is a path in the DAG representation of C from the allocation of q to discard of q', or (ii) q is an input qubit, or q' is an output qubit. Such a dependency prevents reusing q' as q. Notably, each vertex in a QDG has a self-loop.

A recycling strategy $\hookrightarrow$ is valid for C turns out to be equivalent to

$$\to\!\!\hookrightarrow \text{ is acyclic.}$$

Here $\to$ is the edges of $QDG(C)$, and $\to\!\!\hookrightarrow$ is a composed graph where $q \to\!\!\hookrightarrow q''$ if there exists q' such that $q \to q'$ and $q' \hookrightarrow q''$. This criteria is intuitively necessary: a cycle in $\to\!\!\hookrightarrow$ means there is a circular dependency if we are to use this recycling strategy.

The QDG of our running example (Fig. 1a) is shown on the right, where self-loops are omitted for clarity. This QDG hides irrelevant information in the circuit. It is easy to verify that $\{1 \hookrightarrow 2, 2 \hookrightarrow 3\}$ is a valid recycling strategy, while $2 \hookrightarrow 1$ is not due to the presence of a cycle $1 \to 2 \hookrightarrow 1$.

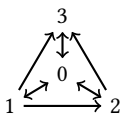

2.2.3 Gap 2: How to Find a Largest Valid Recycling Strategy? Although QDGs provide a more concise criteria of valid recycling strategies, the set of recycling strategies is still quite large, with $O(n!)$ possible injective maps over n qubits, and an even larger number of partial injective maps. Brute-force search becomes unfeasible as the number of qubits grows.

This raises the following natural questions:

(a) Is it possible to efficiently find a largest recycling strategy?
(b) If not, can we find sufficiently good recycling strategies in a reasonable amount of time?

Answering question (a): hardness result. We prove that finding a largest recycling strategy for a QDG is NP-hard. Our key observation is that finding a largest valid strategy for a QDG is equivalent to a matrix triangularization problem. Note that a QDG $\to$ and a recycling strategy $\hookrightarrow$ are directed graphs. Suppose their adjacency matrices are A and R, respectively, then the following holds.

$$\to\!\!\hookrightarrow \text{ is acyclic} \quad \Leftrightarrow \quad AR \text{ is nilpotent} \quad \Leftrightarrow \quad \exists P.\, P^T A(RP) \text{ is strictly lower triangular.} \tag{1}$$

Here P is a permutation matrix. In particular, when R is a total injective map, RP is also a permutation matrix. This equivalent form remind us of another problem: *can a square matrix be made lower (or upper) triangular by independently permuting its rows and columns?*

The problem, known as Wilf's question [Wilf 1997], has been studied extensively in Haddad's dissertation [Haddad 1990], and is known to be NP-complete [Fertin et al. 2015]. We prove that Wilf's question reduces to qubit recycling problem, demonstrating the latter is NP-hard. The main difficulty in this reduction is that the QDG of a circuit is not an arbitrary square 0-1 matrix, for example: it has 1s on its diagonal. The reduction is achieved by appropriately padding a matrix with 0s and 1s, such that it becomes the QDG of some circuit.

Answering question (b): QDG-based algorithms. Based on the previous observation, we develop a solver for this NP-hard problem. The key insight for this solver comes from the triangulation problem: once the permutation P in Eq. (1) is given, a recycling strategy R with maximal size (that

is, the rank of matrix R) can be computed efficiently by putting 0s to the right-upper corner. The problem is then reduced to finding an appropriate permutation P, which can be done either by a heuristic, or by exhaustive search.

We demonstrate the procedure of solving R given P over the adjacency matrix A of the QDG of the circuit in Fig. 1a. The matrix A together with the indices of its rows and columns is shown in Fig. 3a. Suppose we are given a permutation P^T that maps rows 0123 into 3210, then $P^T A$ is shown in Fig. 3b. The solver then try to put the 0s of each row to the right most columns. For example, starting from the first row (with index 3), we put the two 0s to the right, as shown in Fig. 3c. We then continue the process with the remaining submatrix with no background color, that is, we remove the first row, and columns with value 1 in the first row. One more iteration gives the matrix in Fig. 3d, and the procedure stops because no 0s can be found in the remaining submatrix.

	0	1	2	3
0	1	1	1	1
1	1	1	0	1
2	1	0	1	1
3	1	0	0	1

(a)

	0	1	2	3
3	1	0	0	1
2	1	0	1	1
1	1	1	0	1
0	1	1	1	1

(b)

	0	3	2	1
3	1	1	0	0
2	1	1	1	0
1	1	1	0	1
0	1	1	1	1

(c)

	0	3	2	1
3	1	1	0	0
2	1	1	1	0
1	1	1	0	1
0	1	1	1	1

(d)

Fig. 3. Demonstrating the solving procedure using the circuit in Fig. 1a

To get R, we read out the column and row indices of each diagonal elements (in green background) in the strictly lower triangular submatrix at the right upper corner: $(2, 3), (1, 2)$. It coincides with the previous solution $\{1 \hookrightarrow 2, 2 \hookrightarrow 3\}$.

Recall that the solver is parameterized with a permutation P. To find P, it suffices to choose one row at a time, which aligns with the solving procedure. For example, we can choose a row that maximizes the remaining submatrix (greedy), or the number of 0s in the remaining submatrix (heuristics). In addition, we may consult an additional iteration to break a tie (look ahead).

To evaluate the quality of solutions, we also design an ILP model for solving optimal solutions, and an upper-bound estimator for the cases when solving optimal solution is unfeasible. Evaluation (Sec.7.3) over the RevLib [Wille et al. 2008] benchmark shows that these methods can find optimal solutions for most cases.

2.2.4 Generalizing Semantic Preservation. Now that we have an efficient algorithm to find good solutions to the qubit recycling problem, it becomes crucial to ensure the correctness of its implementation. Therefore, we aim to develop a certified qubit recycler that guarantees its correctness. To achieve this, we need to define the correctness for a qubit recycler in the first place.

The correctness of a circuit optimization is typically defined in terms of semantic preservation. However, for qubit recycling, the existing notions of semantic preservation in compiler verification for quantum programs, such as those used in VOQC [Hietala et al. 2021] and Giallar [Tao et al. 2022], do not directly apply.

VOQC's notion of semantic preservation is based on superoperators, with equality defined over the denotations of circuits. However, VOQC explicitly ties qubit identity to their physical location in a density matrix and maintains the dimension of quantum states during execution. This approach makes it challenging to formalize the semantics of dynamic qubit allocation and discard, and it does not support qubit renaming.

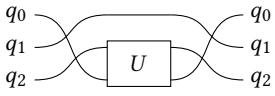

(a) Lifting

$$\frac{C_1 \sqsupseteq C_1' \qquad C_2 \sqsupseteq C_2'}{C_1; C_2 \sqsupseteq C_1'; C_2'} \qquad \frac{C \sqsupseteq C' \qquad C' \sqsupseteq C''}{C \sqsupseteq C''}$$

(b) Compositionality

Fig. 4. Semantic lifting and semantic preservation.

Similarly, Giallar focuses on local unitary rewritings and has a limited notion of semantic preservation for unitary circuits. Since qubit recycling involves non-unitary operations like discard and allocation, their notion of semantic preservation does not directly apply.

Our approach: instrumented circuits, semantic lifting and equivalence. We propose a weaker criterion that allows for qubit renaming and reusing. We achieve this by decoupling qubit identity from their physical location at the beginning or end of execution. This decoupling is accomplished by explicitly instrumenting a circuit C with lists of input/output (I/O) qubits, which serve as maps from qubit identities to their locations in the input/output states.

To define the semantics of a quantum gate with respect to these specific inputs and outputs, we introduce a semantic lifting mechanism. This lifting is defined using permutations and is applied to the qubits before and after the gate operation. For example, when applying a two-qubit unitary gate U on qubits $[q_2, q_0]$ in a state containing qubits $[q_0, q_1, q_2]$, we first permute q_2 and q_0 to adjacent positions, apply the gate U, and then reverse the permutation. Fig. 4a depicts this lifting. This allows us to define semantic preservation that is transitive and congruent to sequential composition.

In our definition of semantic preservation, an instrumented circuit (C', In', Out') preserves the semantics of (C, In, Out), denoted as $C \sqsupseteq C'$ omitting the I/O for short, if there exist bijections f and g (for renaming the qubits), and permutations σ and τ (for positioning the qubits), satisfying:

$$\begin{array}{ccc} In & \xrightarrow{\quad C \quad} & Out \\ \Big\downarrow{\scriptstyle \sigma \circ f} & & \Big\downarrow{\scriptstyle \tau \circ g} \\ In' & \xrightarrow{\quad C' \quad} & Out' \end{array}$$

(1) $\sigma \circ f(In) = In'$, and $\tau \circ g(Out) = Out'$, and
(2) if the input states are equivalent modulo σ, the output states are equivalent modulo τ.

This generalized notion can be roughly interpreted as the above commutative diagram. It allows for qubit renaming and reusing while still preserving the effects on the input and output states modulo permutation. It is congruent with sequential composition and is transitive, as shown in Fig. 4b. This enables modular verification of an optimizer.

In our example, we can observe that the circuit in Fig.1c is semantically equivalent to the circuit in Fig.1a up to certain bijections. Specifically, we have $f = \mathrm{id}$, indicating that the input qubits remain unchanged, and $g = \{3 \mapsto 1, 0 \mapsto 0\}$. The bijection g is uniquely determined by the recycling strategy $1 \hookrightarrow 2, 2 \hookrightarrow 3$. It maps each output qubit $[0; 3]$ of the circuit to their corresponding roots in the graph defined by the recycling strategy. In this case, qubit 3 is mapped to qubit 1, and qubit 0 remains unchanged. This bijection captures the relationship between the output qubits in the original circuit and their corresponding qubits in the optimized circuit, considering the recycling strategy that was applied.

2.2.5 Verification versus Validation? When it comes to building a certified optimizing compiler [Leroy 2009; Rideau and Leroy 2010], we can either directly verify the compiler, or employ an untrusted optimizer alongside a verified validator to validate the result. In the context of qubit recycling, relying solely on verification or validation seems to be unsatisfying. On one hand, verifying the

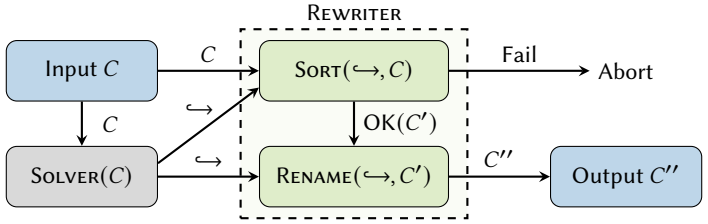

Fig. 5. Structure of the certified qubit recycler.

correctness of the qubit recycler necessitates verifying the previously introduced algorithms concerning QDG, which is time-consuming and sensitive to updates. On the other hand, validation approaches may fall short in terms of completeness, as they may reject correct results. In fact, it is generally impractical to require the validator to be complete: the task of checking the identity of two quantum circuits is generally challenging [Janzing et al. 2003], and existing translation validation methods [Kissinger and van de Wetering 2020] may fail to identify equivalent circuits.

Our approach: integrating verification and validation. We design our optimizer to facilitate the integration of verification and validation techniques, leveraging the benefits of both approaches.

The structure of our certified qubit recycler is illustrated in Fig. 5, each box is a component of the recycler, and the labeled arrows represent the data flowing in and out of the components. Following the decomposition in Sec. 2.2.1, our qubit recycler contains an untrusted Solver (the gray node) that finds recycling strategies, and a verified Rewriter (the green nodes) that rewrites the circuit based on the solver's outputs. The Rewriter takes a circuit C and a recycling strategy $\hookrightarrow$ as its inputs, and either outputs an optimized circuit C'' or aborts indicating $\hookrightarrow$ is invalid.

The Rewriter consists of a Sort module that handles topological deformation (Fig. 2a), and a Rename module that applies the qubit reusing transformation (Fig. 2b). The Sort module is the point where we integrate validation and verification techniques. In essence, Sort performs a topological sorting on a DAG circuit with additional recycling edges, utilizing Kahn's algorithm [Kahn 1962]. Since topological sorting simultaneously sorts the circuit and detects cycles, Sort effectively checks the validity of a recycling strategy while performing topological deformation.

We implemented the Rewriter in Coq, and verified its correctness as both a validator and a circuit rewriter. That is, whenever Rewriter successfully produces a circuit C' from an input $(C, \hookrightarrow)$, then $\hookrightarrow$ is valid w.r.t. C, and the new circuit C' preserves the semantics of C. In addition (but not yet mechanized in Coq), since topological sorting always succeeds on DAGs, the Rewriter will not fail when $\hookrightarrow$ is valid.

3 BASIC SETTINGS

This section presents the syntax of a quantum circuit description language and the qubit recycling problem on it. The instrumented circuits and their semantics are introduced in Sec. 6 when needed.

3.1 Syntax of Quantum Circuits

The left half of Fig. 6 shows the syntax of a simple quantum circuit description language. A (uninstrumented) circuit C is a list of instructions, we use ";" to denote both cons and list concatenation. An *instr* can be one of the followings: **alloc**$[q]$, which allocates a fresh qubit q in state $|0\rangle$; **discard**$[q]$, which measures qubit q and discards the outcome; or $U[\vec{q}]$, which applies a unitary operator U to a list $\vec{q}$ of qubits. The qubit identities range from a set *Qid*. We do not instantiate a gate set, since it

$$
\begin{array}{llcll}
(\textit{Circuit}) & C & ::= & \mathsf{nil} & \textit{instr} \mathbin{\#\#} \textit{instr}' \text{ iff } \textit{args}(\textit{instr}) \cap \textit{args}(\textit{instr}') = \emptyset \\
 & & \mid & \textit{instr}; C & C \mathbin{\#\#} C' \text{ iff } \forall \textit{instr} \in C, \textit{instr}' \in C'.\ \textit{instr} \mathbin{\#\#} \textit{instr}' \\
(\textit{Instr}) & \textit{instr} & ::= & \mathbf{alloc}[q] & \textit{args}(\mathbf{alloc}[q]) = \{q\} \\
 & & \mid & \mathbf{discard}[q] & \textit{args}(\mathbf{discard}[q]) = \{q\} \\
 & & \mid & U[\vec{q}] & \textit{args}(U[\vec{q}]) = \{q \in \vec{q}\}
\end{array}
$$

Fig. 6. Syntax and disjoint instructions.

is mostly irrelevant to qubit recycling. For example, the circuit in Fig. 1a is

$$\mathbf{alloc}[1]; \mathbf{alloc}[2]; \mathbf{alloc}[3]; CX[0,1]; CX[0,2]; CX[0,3]; \mathbf{discard}[1]; \mathbf{discard}[2].$$

The right half of Fig. 6 defines *disjoint* instructions. Two instructions *instr* and *instr′* are disjoint, denoted by *instr* ## *instr′*, if their arguments are disjoint, i.e., $\textit{args}(\textit{instr}) \cap \textit{args}(\textit{instr}') = \emptyset$. Here *args* returns the arguments occurring in an instruction or a circuit. Two circuits C and C' are disjoint, denoted by $C \mathbin{\#\#} C'$, if their instructions are disjoint.

3.2 The Qubit Recycling Problem

When considering the qubit recycling problem, we assume every circuit to be *simple*, that is, a discarded qubit won't be initialized later. For general cases where q is allocated after discard, we may either rename q into a fresh qubit after discard, or combine $\mathbf{discard}[q]$ and $\mathbf{alloc}[q]$ into a measure-and-reset gate, to obtain a simple circuit.

Definition 3.1 (Simple circuits). A circuit C is *simple* if and only if for any $q \in \textit{args}(C)$,

(1) there is at most one $\mathbf{alloc}[q]$ in C, and $\mathbf{alloc}[q]$ (if it exists) is the first gate on q, and
(2) there is at most one $\mathbf{discard}[q]$ in C, and $\mathbf{discard}[q]$ (if it exists) is the last gate on q.

Given an input circuit, the qubit recycling problem is to find a topologically identical circuit that maximizes the number of reusable qubits. We formulate a decision version of this problem to study its complexity. Below we introduce notions used in formalizing the qubit recycling problem.

Reusable qubit. Given two qubits q and q' in a simple circuit C, q' *can reuse* q if and only if $\mathbf{discard}[q]$ occurs before $\mathbf{alloc}[q']$ in C. Formally, q' can reuse q in C if there exists n and n' such that $n < n'$, $C[n] = \mathbf{discard}[q]$ and $C[n'] = \mathbf{alloc}[q']$. Here $C[n]$ is the n-th element in C.

Topologically identical circuits. Two simple circuits C and C' are *topologically identical*, denoted by $C \sim C'$, if we can obtain C' from C by swapping adjacent disjoint instructions:

$$\textsc{Nil}\ \ \mathsf{nil} \sim \mathsf{nil} \qquad \textsc{Skip}\ \ \frac{C \sim C'}{\textit{instr}; C \sim \textit{instr}; C'} \qquad \textsc{Swap}\ \ \frac{\textit{instr} \mathbin{\#\#} \textit{instr}'}{\textit{instr}; \textit{instr}'; C \sim \textit{instr}'; \textit{instr}; C} \qquad \textsc{Trans}\ \ \frac{C \sim C' \qquad C' \sim C''}{C \sim C''}$$

Clearly $\sim$ is an equivalence relation. As we will see in Sec 6, if $C \sim C'$, they are semantically equivalent, so we can safely transform C into C' to find more reusable qubits.

Recycling strategy and validity. We call a set of pairs of qubits $\{(q_i, q_i') \mid i = 1, \ldots k\}$ a *recycling strategy* if it defines an injective partial map over qubits, i.e., for any $i \neq j$ we have $q_i \neq q_j$ and $q_i' \neq q_j'$. The *size* of a recycling strategy is the number of pairs in it. We often use the notation $\hookrightarrow$ for the relation defined by a recycling strategy, i.e., $q_i \hookrightarrow q_i'$ if (q_i, q_i') is in the strategy. A recycling strategy $\hookrightarrow$ is *valid w.r.t.* C, if there exists $C' \sim C$ such that for any $q_i \hookrightarrow q_i'$, q_i' can reuse q_i. Later we will see that a given a valid recycling strategy, we can construct C' in polynomial time.

Definition 3.2 (Qubit recycling problem (decision)). Given a simple circuit C and $k \in \mathbb{N}$, decide if there is a valid recycling strategy w.r.t. C of size k.

The original qubit recycling problem is an optimization problem to find a valid recycling strategy with the largest size. The decision problem in Def. 3.2 reduces to the optimization problem.

4 QUBIT DEPENDENCY GRAPHS

A qubit dependency graph (QDG) makes the qubit recycling problem more manageable. It hides irrelevant details and lets us focus on the computational dependencies that decide whether a qubit can be reused. Below we formalize QDG, then show that the validity of a recycling strategy for a circuit can be determined using its corresponding QDG only. To refer to each instruction in C easily, we implicitly label a instruction by its location in C, such that it is unique in C.

Dependency between instructions. The computation of $instr'$ depends on $instr$ in circuit C, denoted by $instr \prec_C instr'$, if $C = C_1; instr; C_2; instr'; C_3$ such that $(args(instr) \cap args(instr')) - args(C_2)$ is not empty. Equivalently, it means there is an edge from $instr$ to $instr'$ in the DAG representation of C. In particular, if $\mathbf{alloc}[q] \prec_C \mathbf{discard}[q']$, then q cannot reuse q' in any C' such that $C' \sim C$.

Definition 4.1 (Qubit dependency graph). The QDG of a simple circuit C, denoted by $QDG(C)$, is the digraph $(args(C), \rightarrow)$, where $q \rightarrow q'$ if and only if

- q is an input qubit ($\mathbf{alloc}[q] \notin C$), or q' is an output qubit ($\mathbf{discard}[q'] \notin C$), or
- $\mathbf{alloc}[q] \prec_C{}^* \mathbf{discard}[q']$. Here $\prec_C{}^*$ is the reflexive transitive closure of $\prec_C$.

For example, for circuit C in Fig. 1a, we have $1 \rightarrow 2$ in its QDG, because $\mathbf{alloc}[1] \prec_C CX[0,1] \prec_C CX[0,2] \prec_C \mathbf{discard}[2]$; and $0 \leftrightarrow 1$ because $\mathbf{alloc}[0]$ and $\mathbf{discard}[0]$ are not in C.

Notably, QDG is invariant under topological deformation.

Lemma 4.2. *Given simple circuits C and C', if $C \sim C'$, then $QDG(C) = QDG(C')$.*

Proof. It suffices to show swapping a pair of adjacent disjoint instructions does not change instruction dependencies.

Assume $C = C_1; instr; instr'; C_2$, and $C' = C_1; instr'; instr; C_2$, and $instr \ \#\# \ instr'$. We show $a \prec_C b \implies a \prec_{C'} b$ for any a and b, by case study on positions of a and b.

- $a \in C_1$ and $b \in C_2$. Trivial.
- $a = instr$ and $b = instr'$. Thus $args(a) \cap args(b) = \emptyset$, contradicts with $a \prec_C b$.
- $a = instr$ and $C_2 = C_{21}; b; C_{22}$. Since $instr \ \#\# \ instr'$, we have $(args(a) \cap args(b)) - args(instr'; C_{21}) = (args(a) \cap args(b)) - args(C_{21})$. Thus $a \prec_{C'} b$ by definition and $a \prec_C b$.
- $C_1 = C_{11}; a; C_{12}$ and $b = instr'$. Similar to the above case. □

Validity of recycling strategy w.r.t. QDG. A recycling strategy $\hookrightarrow$ is *valid w.r.t a digraph* $(V, \rightarrow)$, if $\hookrightarrow \subseteq V \times V$ and $\rightarrow\hookrightarrow$ is acyclic. Here $v \rightarrow\hookrightarrow v'$ if there is v'' such that $v \rightarrow v''$ and $v'' \hookrightarrow v'$. If $(V, \rightarrow)$ is the QDG of a simple circuit C, the validity of $\hookrightarrow$ w.r.t. C coincides with that w.r.t. QDG.

Lemma 4.3 (Adequacy of QDG). *Given a simple circuit C and a recycling strategy $\hookrightarrow$,*

$$\hookrightarrow \text{ is valid w.r.t } C \iff \hookrightarrow \text{ is valid w.r.t. } QDG(C).$$

Proof. (Sketch)

- "$\Rightarrow$": By validity of $\hookrightarrow$ w.r.t. C, one can construct $C' \sim C$ such that for any $q \hookrightarrow q'$, $\mathbf{discard}[q]$ occurs before $\mathbf{alloc}[q']$ in C'. By Lm. 4.2, it suffices to prove $\hookrightarrow$ is valid w.r.t. $QDG(C')$. We prove this by contradiction. Assume $\rightarrow\hookrightarrow$ is cyclic, i.e., there is q s.t. $q(\rightarrow\hookrightarrow)^+q$. By

definition of $QDG(C')$ and construction of C', we have $\mathbf{alloc}[q]$ occurs before $\mathbf{alloc}[q]$ in C', a contradiction.

- "$\Leftarrow$": It suffices to find $C' \sim C$ such that for any $q \hookrightarrow q'$, $\mathbf{discard}[q]$ occurs before $\mathbf{alloc}[q']$ in C'. This C' can be obtained by topological sorting over instructions in C using $\prec_C \cup \{(\mathbf{discard}[q], \mathbf{alloc}[q']) \mid q \hookrightarrow q'\}$. The above relation is well-defined, because for any $q \hookrightarrow q'$, there exists $\mathbf{discard}[q]$ and $\mathbf{alloc}[q']$ in C, otherwise, say $\mathbf{discard}[q] \notin C$, by definition of QDG, we have $q' \to q \hookrightarrow q'$, contradicts with validity of $\hookrightarrow$ w.r.t. $QDG(C)$. The topological sort must succeed, because the above relation is acyclic, since $\prec_C$ and $\hookrightarrow$ and $\to\hookrightarrow$ are acyclic. Finally, $C' \sim C$ follows from Lm. A.1. □

Validity w.r.t. QDG is irrelevant to *universal vertices*. Here a vertex is universal if it is connected to every vertex in both directions, modeling a qubit that serves as both an input and an output.

Proposition 4.4. *Given a digraph $G = (V, \to)$ and a set $V' \subseteq V$ of universal vertices in G. A recycling strategy is valid w.r.t. G if and only if it is valid w.r.t. the induced subgraph $G[V \setminus V']$.*

5 QUBIT RECYCLING IS NP-HARD

We prove the NP-hardness of the qubit recycling problem by showing the corresponding decision problem (Def. 3.2) is NP-complete. This proof involves two reductions, with recycling on QDGs (Definition 5.2) serving as the link between an NPC problem and the qubit recycling problem.

Theorem 5.1. *The decision version of the qubit recycling problem is NP-complete.*

Proof. The qubit recycling problem is in NP, because detecting cycles in a digraph has linear time algorithms. To show it is NP-complete, it suffices to prove the following reductions, since Wilf's question is NP-complete [Fertin et al. 2015].

Wilf's question	$\leq_p$	Recycling on QDGs	$\leq_p$	Qubit recycling
(Def. 5.6)	(Lm. 5.7,5.5)	(Def. 5.2)	(Lm. 5.3)	(Def. 3.2)

□

In the following subsections, we explain the reduction steps from right to left.

5.1 Recycling on QDGs Reduces to Qubit Recycling

We first formalize the intermediate problem using QDG. Observe from Def. 4.1 that for each qubit q occurs in C, $q \to q$ in $QDG(C)$, we consider digraph with self loops only.

Definition 5.2 (Recycling problem on QDG). Given a digraph $G = (V, \to)$ such that $\forall v \in V. v \to v$, and a natural number $k > 0$, decide whether there is a valid recycling strategy of size k w.r.t. G.

To reduce Def. 5.2 to qubit recycling problem, we construct a circuit based on a digraph $(V, \to)$ using Alg. 1. The intuition is that for each edge $e = (v, v')$, we introduce a fresh qubit $\hat{v}_e$ and two CX gates, such that $\mathbf{alloc}[v] \prec CX[v, \hat{v}] \prec CX[v', \hat{v}] \prec \mathbf{discard}[v']$, i.e., $v \to v'$ is also in the constructed circuit's QDG. Since $\hat{v}$ are I/O qubits, they are universal vertices, and do not introduce new valid recycling strategies.

For example, in Fig. 7, the left-most of is a 3-node digraph, in the middle is the constructed circuit. The right-most is the QDG of the circuit, for clarity, we

Algorithm 1 ConstructCirc$(V, \to)$

```
C ← nil
for e ∈ {(v, v') | v → v' ∧ v ≠ v'} do
    C ← CX[v, v̂_e]; C; CX[v', v̂_e]
    // v̂_e is fresh
end for
for v ∈ V do
    C ← alloc[v]; C; discard[v]
end for
return C
```

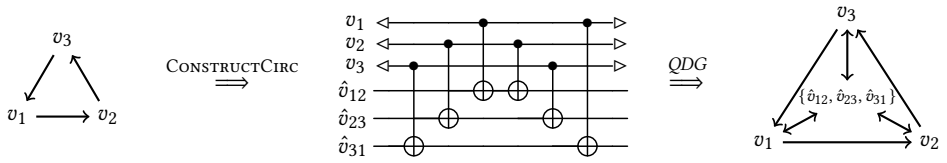

Fig. 7. An example digraph and the constructed circuit. Self loops are omitted.

merge the $\hat{v}$ vertices. A recycling strategy is valid w.r.t. the left-most digraph if and only if it is valid w.r.t. the right most digraph, since $\hat{v_{ij}}$ are universal vertices.

Lemma 5.3. *The recycling problem on QDGs reduces to qubit recycling.*

Proof. Given digraph $G = (V, \rightarrow)$ such that $\forall v \in V. v \rightarrow v$, we construct an instance $C = \textsc{ConstructCirc}(G)$ of the qubit recycling problem. The construction is of polynomial time w.r.t. the size of G. The resulting circuit C is simple, and each gate in C is unique.

To prove the goal, it suffices to show that for any recycling strategy $\hookrightarrow$, its validity w.r.t. G is equivalent to that w.r.t. C:

$$\hookrightarrow \text{ valid w.r.t. } C \overset{\text{(Lm. 4.3)}}{\iff} \hookrightarrow \text{ valid w.r.t. } QDG(C) \overset{\text{(Prop. 4.4)}}{\iff} \hookrightarrow \text{ valid w.r.t. } QDG(C)[V] = G.$$

The right most equal sign follows from Lm. A.4. □

5.2 Wilf's Question Reduces to Recycling on QDGs

We rephrase Def. 5.2 using adjacency matrices, and observe that a digraph is acyclic if and only if its adjacency matrix A can be made strictly upper triangular by permuting its columns and rows simultaneously. That is, there is a permutation matrix P such that $P^T AP$ is strictly upper triangular.

Definition 5.4 (A triangularization problem). Given a square 0, 1-matrix A whose diagonal elements are all 1s, and a natural number $k > 0$, decide if there exists permutation matrices P and Q such that $PAQ = \left[\begin{smallmatrix} * & B \\ * & * \end{smallmatrix}\right]$ for some $k \times k$ strictly lower-triangular matrix B.

We show that the formulation in Def. 5.4 is equivalent to Def 5.2.

Lemma 5.5. *Recycling problem on QDGs is equivalent to the triangularization problem (Def. 5.4).*

Proof. Recall that a recycling strategy $\hookrightarrow$ of size k defines an injective partial map over qubits. Thus its corresponding adjacency matrix R is a partial permutation matrix of rank k, that is, there exists permutation matrices P and Q such that $R = Q \left[\begin{smallmatrix} I_k & 0 \\ 0 & 0 \end{smallmatrix}\right] P$, where I_k is the identity matrix of order k. Also observe that given $G = (V, \rightarrow)$ and its adjacency matrix A, the graph on V defined by $\rightarrow\hookrightarrow$ has adjacency matrix AR.

Together with the fact that a digraph is acyclic iff its adjacency matrix is nilpotent, we rephrase the recycling problem on QDGs: given adjacency matrix A whose diagonal elements are all 1s and $k \in \mathbb{N}$, decide whether there exist permutations P, Q such that $AQ \left[\begin{smallmatrix} I_k & 0 \\ 0 & 0 \end{smallmatrix}\right] P$ is nilpotent.

The rest of the proof is shown below, where P, Q are permutation, and B is of order k.

$$\begin{aligned}
& \exists P, Q.\, PAQ = \left[\begin{smallmatrix} * & B \\ * & * \end{smallmatrix}\right] \text{ for some strictly lower-triangular matrix } B \\
\Leftrightarrow\ & \exists P, Q.\, PAQ = \left[\begin{smallmatrix} B & * \\ * & * \end{smallmatrix}\right] \text{ for some nilpotent matrix } B && \text{(By Lemma A.5)} \\
\Leftrightarrow\ & \exists P, Q.\, PAQ \left[\begin{smallmatrix} I_k & 0 \\ 0 & 0 \end{smallmatrix}\right] PP^T = \left[\begin{smallmatrix} * & 0 \\ * & 0 \end{smallmatrix}\right] \text{ is nilpotent} \\
\Leftrightarrow\ & \exists P, Q.\, AQ \left[\begin{smallmatrix} I_k & 0 \\ 0 & 0 \end{smallmatrix}\right] P \text{ is nilpotent.}
\end{aligned}$$

□

The formulation in Def. 5.4 is close enough to Wilf's question defined below.

Definition 5.6 (Wilf's question [Wilf 1997]). Given a square 0, 1-matrix A, Wilf's question, denoted by $\textsc{Wilf}(A)$, asks the existence of permutations P and Q such that PAQ is upper triangular.

Lemma 5.7. *Wilf's question reduces to the triangularization problem.*

Given an instance of Wilf's question, we can construct a matrix as an instance of problem Def. 5.4 that has the same answer. The construction is by appropriately padding a matrix with 0s and 1s. The detailed proof of Lm. 5.7 is in Appendix B.

6 CERTIFIED QUBIT RECYCLER

This section presents the verified qubit recycler

$$\textsc{Rewriter}(\hookrightarrow, \widetilde{C}) ::= (\textsc{Rename}(\hookrightarrow, -) \circ \textsc{Sort}(\hookrightarrow, -))(\widetilde{C}).$$

We break down the correctness proof into syntactic and semantic properties, as shown below.

$$\textsc{Rewriter}(\hookrightarrow, \widetilde{C}) = \mathsf{OK}(\widetilde{C'}) \overset{\text{(Lm. 6.4,6.5,6.7)}}{\Longrightarrow} \widetilde{C} \rightarrowtail^* \widetilde{C'} \overset{\text{(Lm. 6.3,6.2)}}{\Longrightarrow} \widetilde{C} \sqsupseteq \widetilde{C'}$$

The philosophy is to break down semantic preservation in a way that minimizes semantic properties by replacing them with syntactic ones wherever possible. This approach stems from the fact that syntactic properties are often considerably easier to prove than semantic ones.

Syntactically, we establish that (i) $\textsc{Sort}(-, \widetilde{C})$ is a correct validator for the validity of a recycling strategy; and (ii) when $\hookrightarrow$ is a valid recycling strategy, $\textsc{Sort}(\hookrightarrow, -)$ and $\textsc{Rename}(\hookrightarrow, -)$ equates to a series of atomic circuit rewrites ($\rightarrowtail$). Semantically, we demonstrate that these rewrites preserve semantics ($\sqsupseteq$), akin to a soundness proof of rewrite rules.

In the subsequent subsections, we first introduce instrumented circuits that incorporate Input/Output qubits, along with their denotational semantics and semantic preservation between different instrumented circuits. Following this, we present two atomic circuit rewrites and establish the soundness of the associated rewriting rules. Lastly, we provide a brief overview of the implementation of Rewriter components and establish their syntactic properties. Results presented in this section are formalized in Coq, unless explicitly stated otherwise.

6.1 Instrumented Circuits and Semantic Preservation

6.1.1 Instrumented circuits. To decouple qubit identities from their locations and support dynamic qubit allocation/discard, we instrument a circuit with lists of I/O qubits, which serve as maps from qubit to its locations. These I/O qubit lists should be consistent with the instructions in the circuit.

Formally, the instrumented circuits, denoted by $C : \mathit{In} \rightsquigarrow \mathit{Out}$[1], is inductively defined as follows.

$$\frac{\mathsf{NoDup}(\mathit{In}) \qquad \mathit{In} \equiv_p \mathit{Out}}{\mathsf{nil} : \mathit{In} \rightsquigarrow \mathit{Out}} \qquad \frac{\mathsf{NoDup}(\vec{q}) \qquad \vec{q} \subseteq \mathit{In} \qquad C : \mathit{In} \rightsquigarrow \mathit{Out}}{U[\vec{q}]; C : \mathit{In} \rightsquigarrow \mathit{Out}}$$

$$\frac{q \in \mathit{In} \qquad C : \mathit{In} \rightsquigarrow \mathit{Out}}{\mathbf{alloc}[q]; C : \mathit{In} \setminus \{q\} \rightsquigarrow \mathit{Out}} \qquad \frac{q \in \mathit{In} \qquad C : \mathit{In} \setminus \{q\} \rightsquigarrow \mathit{Out}}{\mathbf{discard}[q]; C : \mathit{In} \rightsquigarrow \mathit{Out}}$$

Here $A \equiv_p B$ means list A is a permutation of list B.

Intuitively, the I/O list of qubits represents the *living* qubit at the beginning/end of the circuit, respectively. An empty circuit or a unitary gate does not change living qubits. An $\mathbf{alloc}[q]$ instruction brings a dead qubit q alive, while $\mathbf{discard}[q]$ kills an alive q. Instructions other than $\mathbf{alloc}[q]$ must operate on living qubits. We often denote $(C : \mathit{In} \rightsquigarrow \mathit{Out})$ by $\widetilde{C}$ when In and Out are irrelevant.

[1]In our Coq development, an instrumented circuit is a triple $(C, \mathit{In}, \mathit{Out})$ that satisfies a similarly defined property.

6.1.2 Denotational Semantics. We consider a symmetric monoidal category as the semantic domain. It serves as a comprehensive library of axioms for the semantic domain, isolating elements that are directly relevant to our objectives from the intricacies of lower-level representations such as density matrices and superoperators.

Concretely, we follow [Selinger 2004], where the semantic domain is a category of superoperators. Since our focus is on the symmetric monoidal structure, we do not assume a concrete category instance. Below we introduce a specific instantiation, **SuperOp**, to aid in understanding.

Semantic domain: symmetric monoidal categories. The objects of **SuperOp** are natural numbers. Each object n can be interpreted as the number of qubits in a system, or the Hilbert space $\mathcal{H}_{2^n}$ where an n-qubit system resides in. Special objects in **SuperOp** includes $\mathbf{I} = 0$, and $\mathbf{qbit} = 1$. A morphism from m to n is a superoperator $\mathcal{E} : \mathcal{H}_{2^m} \to \mathcal{H}_{2^n}$.

Additionaly, **SuperOp** has a symmetric monoidal structure. The product $\otimes$ over objects m and n is defined as $m+n$. The unit of this product is the object $\mathbf{I} = 0$. Given morphisms $\mathcal{E}_1 \in \mathrm{Hom}(m_1, n_1)$, and $\mathcal{E}_2 \in \mathrm{Hom}(m_2, n_2)$, the product $\otimes$ over morphisms $\mathcal{E}_1 \otimes \mathcal{E}_2 \in \mathrm{Hom}(m_1 \otimes m_2, n_1 \otimes n_2)$ is defined on a basis elements $e_1 \otimes e_2$ via $(\mathcal{E}_1 \otimes \mathcal{E}_2)(e_1 \otimes e_2) = \mathcal{E}_1(e_1) \otimes \mathcal{E}_2(e_2)$, and extends to arbitrary elements by linearity. Finally, the twist β is defined on basis elements $e_1 \otimes e_2$ via $\beta(e_1 \otimes e_2) = e_2 \otimes e_1$.

Using the category **SuperOp**, the denotation of each individual instruction is shown below, originally formalized in [Selinger 2004]. A qubit q is associated with the object **qbit**: $[\![q]\!] = \mathbf{qbit}$; and a list of n qubits is associated with the tensor product of **qbit**s: $[\![\vec{q}]\!] = [\![\vec{q}[1]]\!] \otimes \ldots \otimes [\![\vec{q}[n]]\!] = \mathbf{qbit}^n$. In particular, an empty list of qubits nil is associated with the tensor unit: $[\![\mathsf{nil}]\!] = \mathbf{I}$.

$$
\begin{aligned}
[\![\mathbf{alloc}[q]]\!] \in \mathrm{Hom}([\![\mathsf{nil}]\!], [\![[q]]\!]) \quad &: \quad a \mapsto \left[\begin{smallmatrix} a & 0 \\ 0 & 0 \end{smallmatrix}\right] \\
[\![\mathbf{discard}[q]]\!] \in \mathrm{Hom}([\![[q]]\!], [\![\mathsf{nil}]\!]) \quad &: \quad \left[\begin{smallmatrix} a & b \\ c & d \end{smallmatrix}\right] \mapsto a + d \\
[\![U[\vec{q}]]\!] \in \mathrm{End}([\![\vec{q}]\!]) \quad &: \quad A \mapsto UAU^\dagger \\
\mathit{permute}_\sigma \in \quad \mathrm{Hom}(X_1 \otimes X_2 \otimes \ldots \otimes X_n, \;& X_{\sigma(1)} \otimes X_{\sigma(2)} \otimes \ldots \otimes X_{\sigma(n)})
\end{aligned}
$$

Here, we also introduce a family of special morphisms $\mathit{permute}_\sigma$ for later defining semantic lifting. This is the natural permutation map based on the symmetric tensor $\otimes$.

We further generalize our semantic domain to an arbitrary symmetric monoidal category, since a symmetrical monoidal structure is sufficient for proving correctness of qubit recycling. We refer to the book [Etingof et al. 2016] for more details about symmetric monoidal categories. This generalization is reasonable because, commonly used semantic domains for quantum programs [Abramsky and Coecke 2004; Heunen and Vicary 2019; Selinger 2004, 2005] share a symmetric monoidal structure. Notably, by encoding permutations as twists within an SMC, their properties and interactions with tensor product or other morphisms are succinctly captured by the coherence identities. This enables us to avoid repeatly dealing with matrix representations of permutations and cubersome index manipulations in Kronecker products. The remainder contents of this section depends only on the properties of a symmetric monoidal category, without referring to the concrete instantiation **SuperOp**.

In detail, we parameterize over an arbitrary symmetric monoidal category **SMC** as the semantic domain, and assume a special object $\mathbf{qbit} \in \mathbf{SMC}$. In defining denotations for **alloc** and **discard**, we assume morphisms $\mathit{alloc} \in \mathrm{Hom}(\mathbf{I}, \mathbf{qbit})$ and $\mathit{discard} \in \mathrm{Hom}(\mathbf{qbit}, \mathbf{I})$. For unitary operations, we assume a partial map $\mathit{unitary}(U, n) : \mathrm{End}(\mathbf{qbit}^n) \cup \{\bot\}$, where an endomorphism is defined only if U can be applied over n qubits. The $\mathit{permute}_\sigma$ morphism generalizes to any morphism in **SMC** that implements the permutation σ, constructed using associator $\alpha_{X,Y,Z} : (X \otimes Y) \otimes Z \cong X \otimes (Y \otimes Z)$, left and right unitors $\lambda_X : \mathbf{I} \otimes X \cong X$ and $\rho_X : X \otimes \mathbf{I} \cong X$, or twist $\beta_{X,Y} : X \otimes Y \cong Y \otimes X$. By the

$$
\begin{aligned}
[\![\mathsf{nil} : \mathit{In} \rightsquigarrow \mathit{Out}]\!] &= \mathit{permute}_{\sigma} && \text{where } \mathit{Out} = \sigma(\mathit{In}) \\
[\![\mathbf{alloc}[q] : \mathit{In} \rightsquigarrow \mathit{Out}]\!] &= \mathit{permute}_{\sigma} \circ \mathit{alloc} \otimes \mathsf{id} \circ \lambda^{-1} && \text{where } \mathit{Out} = \sigma(q; \mathit{In}) \\
[\![\mathbf{discard}[q] : \mathit{In} \rightsquigarrow \mathit{Out}]\!] &= \lambda \circ \mathit{discard} \otimes \mathsf{id} \circ \mathit{permute}_{\sigma} && \text{where } q; \mathit{Out} = \sigma(\mathit{In}) \\
[\![U[\vec{q}] : \mathit{In} \rightsquigarrow \mathit{Out}]\!] &= \mathit{permute}_{\tau} \circ \mathit{unitary}(U, |\vec{q}|) \otimes \mathsf{id} \circ \mathit{permute}_{\sigma} \\
&\qquad \text{where } \sigma(\mathit{In}) = (\vec{q}; \mathit{Mid}) = \tau^{-1}(\mathit{Out}) \text{ for some } \mathit{Mid} \\
[\![C_1; C_2 : \mathit{In} \rightsquigarrow \mathit{Out}]\!] &= [\![C_2 : \mathit{Mid} \rightsquigarrow \mathit{Out}]\!] \circ [\![C_1 : \mathit{In} \rightsquigarrow \mathit{Mid}]\!] && \text{for some } \mathit{Mid}
\end{aligned}
$$

Fig. 8. Lifted semantics

coherence theorem of symmetric monoidal categories, these morphisms are identical, thus the generalized $\mathit{permute}_{\sigma}$ is well defined.

Semantic lifting. On top of an **SMC** and the parameterized objects and morphisms, we define the denotation of an instrumented circuit ($C : \mathit{In} \rightsquigarrow \mathit{Out}$) by lifting the morphisms of individual instructions to a morphism between the I/O qubits, using permutation and left/right unitors. This is to permute the input qubits *In* to make the arguments of an instruction adjacent and aligned in order, such that the morphisms of the corresponding instruction is applicable. After applying the morphism, we again permutes the living qubits such that they are in the order defined by *Out*.

The denotational semantics lifted w.r.t. I/O is formalized in Fig. 8. We omit the associators for clarity, since they are irrelevant by the coherence theorem of a monoidal category. A denotation is defined only if the intermediate terms are all defined. The permutations involved are uniquely determined, and the choice of the intermediate qubit lists *Mid* does not affect the results. Thus Fig. 8 indeed defines a partial function over the instrumented circuits.

Graphical representations for the lifted denotation of **alloc**, **discard** and U are depicted in Fig. 9. An arrow represents an object (or the identity morphism) in **SMC**, which is labeled next to the line. The object **I** is specially represented by a dashed arrow. Arrows placed in juxtaposition means a tensor product of objects. A morphism is represented by a box or triangle, whose domain is the line coming from the bottom, and the codomain is the line outgoing to the top.

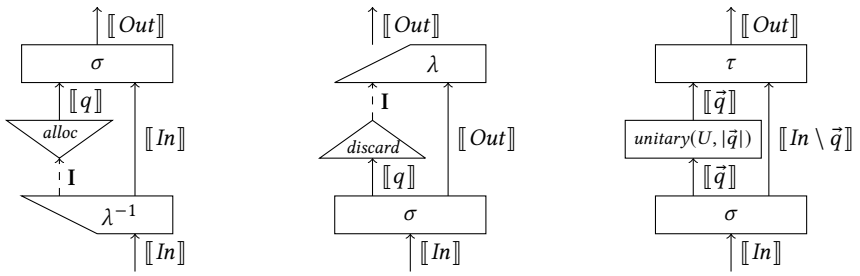

(a) $[\![\mathbf{alloc}[q] : \mathit{In} \rightsquigarrow \mathit{Out}]\!]$ (b) $[\![\mathbf{discard}[q] : \mathit{In} \rightsquigarrow \mathit{Out}]\!]$ (c) $[\![U[\vec{q}] : \mathit{In} \rightsquigarrow \mathit{Out}]\!]$

Fig. 9. Graphical repr. of the lifting. Here λ is the left unitor, σ and τ are permutation morphisms.

6.1.3 Semantic Preservation. On top of the denotational semantics, semantic preservation is naturally defined as equivalence over the denotations modulo renaming and permutation.

Definition 6.1 (Semantic preservation). For any instrumented circuits $C : In \rightsquigarrow Out$ and $C' : In' \rightsquigarrow Out'$, the latter preserves the semantics of the former, denoted as $\widetilde{C} \sqsupseteq \widetilde{C'}$, if there exists bijections f, g, and permutations σ, τ, such that

(1) (I/O equivalence up to renaming and permutation) $In' = \sigma \circ f(In)$ and $\tau(Out') = g(Out)$; and
(2) (Safety preservation) if $[\![\widetilde{C}]\!]$ is defined, then $[\![\widetilde{C'}]\!]$ is defined; and
(3) (Semantics equivalence modulo permutation) $[\![\widetilde{C}]\!] = permute_{\tau} \circ [\![\widetilde{C'}]\!] \circ permute_{\sigma}$.

We prove that this semantic preservation is compositional.

Lemma 6.2 (Compositionality). *The relation $\sqsupseteq$ is transitive, and is congruent to sequential composition. The latter is, for any $\widetilde{C_1}, \widetilde{C'_1}, \widetilde{C_2}, \widetilde{C'_2}$, we have $\widetilde{C_1} \sqsupseteq \widetilde{C'_1} \wedge \widetilde{C_2} \sqsupseteq \widetilde{C'_2} \implies \widetilde{C_1}; \widetilde{C_2} \sqsupseteq \widetilde{C'_1}; \widetilde{C'_2}$. Here $\widetilde{C}; \widetilde{C'}$ is defined only if there is a Mid such that $\widetilde{C} = (C : In \rightsquigarrow Mid)$ and $\widetilde{C'} = (C' : Mid \rightsquigarrow Out)$.*

6.2 Rewriting rules

We introduce two rewriting rules over instrumented circuits, and use relation $\widetilde{C} \rightarrowtail \widetilde{C'}$ to denote $\widetilde{C'}$ is obtained from $\widetilde{C}$ via a rewriting step.

TopoDeform
$$\frac{In \equiv_p In' \qquad C \sim C' \qquad Out \equiv_p Out'}{(C : In \rightsquigarrow Out) \rightarrowtail (C' : In' \rightsquigarrow Out')}$$

Reuse
$$\frac{q' \notin (C_1 : In \rightsquigarrow Mid) \qquad q \notin (C_2 : Mid \rightsquigarrow Out)}{(C_1; C_2 : In \rightsquigarrow Out) \rightarrowtail (C_1; C_2 : In \rightsquigarrow Out)[q/q']}$$

Here $q \notin (C : In \rightsquigarrow Out)$ indicates that qubit q is not present in the sets In and Out, nor is it used as an argument in any instructions within C. This signifies that q is entirely irrelevant in the instrumented circuit, and its lifetime does not overlap with the execution of C. The notation $[q/q']$ denotes the substitution of each occurrence of q' with q.

The first rule involves topological deformation, and permits permutation on I/O qubits, while the second rule allows for the reuse of qubit q as q', given that the lifetime of q precedes that of q'.

We prove that these rewriting rules are sound. The proof relies on properties such as the interchange law and coherence theorem of a symmetric monoidal category.

Lemma 6.3 (Soundness of rewriting rules). *If $\widetilde{C} \rightarrowtail \widetilde{C'}$, then $\widetilde{C} \sqsupseteq \widetilde{C'}$.*

In the following subsections, we show that the overall behavior of our recycler is equivalent to a series of circuit rewritings using these two rules.

6.3 Sorting and Validity Checking

The Sort function takes a recycling strategy $\hookrightarrow$ and a circuit C as inputs. It tries to do topological deformation over C such that the reordered circuit C' is compatible with $\hookrightarrow$. That is, for each $q \hookrightarrow q'$, q' can reuse q in C'.

The algorithm Sort is outlined in Alg. 2. In line 1, the algorithm first checks two conditions for the input $\hookrightarrow$: (i) $\hookrightarrow$ is an injective function, and (ii) for each $q \hookrightarrow q'$, both $\mathbf{discard}[q]$ and $\mathbf{alloc}[q]$ are present in C. If both conditions are met, the circuit is translated into a DAG representation, denoted as G (line 2). Next, edges $(\mathbf{discard}[q], \mathbf{alloc}[q'])$ are added to G for each $q \hookrightarrow q'$, resulting in G' (line 3). The algorithm then performs a topological sorting using Kahn's algorithm (line 4). Kahn's algorithm guarantees that the circuit is reordered without violating computational dependencies, ensuring that $\mathbf{discard}[q]$ occurs before $\mathbf{alloc}[q']$ for each $q \hookrightarrow q'$. If the topological

sorting succeeds, the algorithm returns the reordered circuit (line 5); otherwise, it detects a cycle in G' that invalidates $\hookrightarrow$.

The following lemma states that if Sort succeeds, it produces a topological deformation on the input circuit, which, in turn, corresponds to an atomic rewriting.

Algorithm 2 Sort$(\hookrightarrow, \widetilde{C})$

1: **if** $\hookrightarrow$ is a recycling strategy for C **then**
2: $G \leftarrow$ DAG of C
3: $G' \leftarrow G$ with edges defined by $\hookrightarrow$
4: **if** *TopoSort*(G') = OK(C') **then**
5: **return** OK$(C' : \mathit{In} \rightsquigarrow \mathit{Out})$
6: **end if**
7: **end if**
8: **return** Invalid recycling strategy

Lemma 6.4 (Sort returns a topological deformation of C.). *Given $C : \mathit{In} \rightsquigarrow \mathit{Out}$ and $\hookrightarrow$, if* Sort$(\hookrightarrow, (C : \mathit{In} \rightsquigarrow \mathit{Out})) = \mathit{OK}(C' : \mathit{In} \rightsquigarrow \mathit{Out})$*, then $C' \sim C$. By definition, $\widetilde{C} \rightarrowtail \widetilde{C'}$.*

As mentioned in Sec. 2.2, Sort also serves as a validator for the validity of $\hookrightarrow$. The following lemma states its correctness as a validator, which guarantees $\hookrightarrow$ is a correct input for the subsequent phase Rename.

Lemma 6.5 (Sort is a correct validator). *Given $\widetilde{C}$ and $\hookrightarrow$, if* Sort$(\hookrightarrow, \widetilde{C}) = \mathit{OK}(\widetilde{C'})$ *for some C', then for any $q \hookrightarrow q'$, q' can reuse q in C'.*

The inverse of the previous lemma also holds, which says Sort is a "complete" validator.

Lemma 6.6 (Sort succeeds when recycling strategy is valid). *Given $\widetilde{C}$ and $\hookrightarrow$, then $\hookrightarrow$ is valid w.r.t. C if and only if* Sort$(\hookrightarrow, \widetilde{C})$ *succeeds.*

The proof of Lm. 6.6 is straightforward, but not yet mechanized in Coq.

Proof. Recall that edges of the DAG representation of C are dependencies $\prec_C$ between instructions. It is straightforward to show that if $C' \sim C$, then C' is a topological sorting of the DAG of C. By definition, $\hookrightarrow$ is valid w.r.t. C if and only if there is a topological sorting C' of the DAG of C which is additionally compatible with the order $\{(\mathbf{discard}[q], \mathbf{alloc}[q']) \mid q \hookrightarrow q'\}$. I.e., there is a topological sorting C' of the DAG of C with additional edges $\{(\mathbf{discard}[q], \mathbf{alloc}[q']) \mid q \hookrightarrow q'\}$. Kahn's algorithm succeeds if and only if this topological sorting exists. □

6.4 Reusing by Renaming

Algorithm 3 Rename$(\hookrightarrow, \widetilde{C})$

1: **if** $\hookrightarrow = \{(q, q')\} \cup \hookrightarrow'$ **then**
2: **return** Rename$(\hookrightarrow' [q/q'], \widetilde{C}[q/q'])$
3: **else**
4: **return** $\widetilde{C}$
5: **end if**

The Rename function is described in Alg. 3. It operates by removing a pair of qubits (q, q') from the recycling strategy $\hookrightarrow$. Subsequently, it performs a substitution (line 4), replacing all occurrences of q' with q in the remaining part of $\hookrightarrow$ and the instrumented circuit $\widetilde{C}$. The function proceeds to recursively invoke Rename on the updated recycling strategy and instrumented circuit, thus continuing the recycling process.

Intuitively, in each iteration of the substitution process in line 4, a single qubit is reused. Notably, Rename is a total function, it preserves semantics only if the inputs are appropriate. The following lemma establishes that when the recycling strategy $\hookrightarrow$ is valid, the Rename function is equivalent to a series of atomic rewrites (using the Reuse rule) over the instrumented circuit $\widetilde{C}$.

Algorithm 4 Solver(f, A, σ)

if not $halt(\sigma)$ **then**
  $r \leftarrow f(A, \sigma)$
  $\sigma \xrightarrow{r}_A \sigma'$
  Solver(f, A, σ')
else return Extract(σ)
end if

Algorithm 5 Extract(σ)

$rl \leftarrow \sigma$.rows
$k \leftarrow |rl|$
$cl \leftarrow \sigma$.cols_del ++σ.cols
return $\{(cl[n-k+i], rl[i]) \mid i = 0, 1, ..., k-1\}$

Lemma 6.7 (Rename is equivalent to a series rewrites). *For any $\hookrightarrow$ and $\widetilde{C}$, if q' can reuse q in C for any $q \hookrightarrow q'$, then $\widetilde{C} \rightarrowtail^* \textit{Rename}(\hookrightarrow, \widetilde{C})$.*

6.5 Final Theorem and Coq Development

Putting the previous results together, we obtain the final theorem for our certified qubit recycler.

Theorem 6.8. *For any recycling strategy $\hookrightarrow$ and instrumented circuits $\widetilde{C}$ and $\widetilde{C}'$,*

$$\textit{Rewriter}(\hookrightarrow, \widetilde{C}) = \mathsf{OK}(\widetilde{C}') \implies \widetilde{C} \sqsupseteq \widetilde{C}'.$$

We implemented Rewriter and mechanized Thm. 6.8 in the Coq proof assistant, with ~6k lines of Coq code. The mechanization is built on top of an axiom-free formalization of category theory in Coq [Wiegley 2022]. Notable byproducts of this Coq formalization include the implementation and verification of Kahn's algorithm for topological sorting, and version of the coherence theorem for symmetric monoidal categories.

We extracted Rewriter to OCaml such that it can work together with the Solver in Sec. 7.

7 SOLVER FOR FINDING RECYCLING STRATEGIES

This section presents our algorithm for finding recycling strategies, and an empirical evaluation on the RevLib [Wille et al. 2008] benchmark.

7.1 The Algorithm

Our algorithm is outlined in Alg. 4. The Solver is inspired by Lm. 5.5, that finding recycling strategies on QDGs is equivalent to a triangularization problem. The Solver is essentially a polynomial time algorithm for the triangularization problem given a row permutation P. It implements the procedure demonstrated in Fig. 3: given a heuristic function f (which essentially computes a permutation P one row at a time), an $n \times n$ matrix A representing a QDG, and a current state σ, it iteratively choose a row r using f, take a step to state σ', and continue the procedure.

A state σ is a tuple (rows, cols, cols_del, k). Here rows is a list of row indices already chosen, cols is the list of remaining columns, cols_del is the list of deleted columns, and k is an upper-bound of the number of further steps.

The initial state is $\sigma_0 = ([], [0, ..., n-1], [], n)$, and $halt(\sigma)$ if σ.k ≤ 0. The stepping rule is:

$$\frac{r \notin \texttt{rows} \qquad \texttt{cols}' = \texttt{cols} \backslash \{j \mid A_{rj} = 1\} \qquad \texttt{cols\_del}' = \texttt{cols\_del} \mathbin{+\!\!+} (\texttt{cols} \backslash \texttt{cols}') \qquad \texttt{rows}' = (\texttt{cols}' = [] \ ?\ \texttt{rows} : (\texttt{rows} \mathbin{+\!\!+} [r])) \qquad \texttt{k}' = \min(\texttt{k}, |\texttt{cols}'|) - 1}{(\texttt{rows}, \texttt{cols}, \texttt{cols\_del}, \texttt{k}) \xrightarrow{r}_A (\texttt{rows}', \texttt{cols'}, \texttt{cols\_del}', \texttt{k}')}$$

In each step, given a next row r, it deletes those columns j such that $A_{rj} = 1$, and updates the list for remaining columns (col) and deleted columns (col_del). It then appends r to rows if the remaining columns col' is not empty. Finally, it updates k to the minimum of k − 1 and |cols′| − 1.

When reaching a halting state σ_h, the solver extracts the solution from σ_h, as described in Alg. 5. The size of the extracted recycling strategy is the number of overall steps.

Below we illustrate an execution of this algorithm using the QDG presented in Sec. 2.2 as an example. We assume the heuristic f chooses rows $(3, 2, 1, 0)$ in order.

	0	1	2	3
0	1	1	1	1
1	1	1	0	1
2	1	0	1	1
3	1	0	0	1

	r	row	col	col_del	k
σ_0	3	[]	$[0, 1, 2, 3]$	[]	4
σ_1	2	$[3]$	$[1, 2]$	$[0, 3]$	1
σ_2	–	$[3, 2]$	$[1]$	$[0, 3, 2]$	-1

The algorithm halts after 2 steps. Extracting the result from σ_2 yields $\{(2, 3), (1, 2)\}$, a solution of size 2 and coincides with our previous solution.

We also adapted the "dual-circuit" technique [DeCross et al. 2023], which appears to be more intuitive in our settings. Recall that a valid recycling strategy w.r.t. a QDG A is essentially a partial permutation matrix R such that AR is nilpotent, it is straightforward to show that R^T is a valid recycling strategy w.r.t. A^T. We apply the solver to both A and A^T, and return the larger solution.

7.1.1 Designs of the Heuristics. It remains to find an appropriate heuristic f such that the number of overall steps is maximized. We design heuristics based on the following observations:

(1) (`Greedy`) The bound `k` in the state strictly decreases as the algorithm proceeds, and the algorithm halts if `k` ≤ 0. Therefore, we may choose the next row that maximizes the bound `k` in the next step, such that the algorithm is likely to step more.
(2) (`Max0s`) The more 0s there are in the submatrix A`[rows′][cols′]`, it is more likely for the algorithm to continue stepping. Therefore, we may choose the next row that maximizes the number of 0s in A`[rows′][cols′]`.
(3) (`LA`) In experiments, it is common that several rows perform equally. In these cases, we may break a tie by taking a further step (look-ahead).

Later in this section, we evaluate these heuristics, which yield optimal results most of the time.

7.2 An ILP Model and Upper-Bound Estimator for Qubit Recycling

To tell whether our heuristics obtain an optimal solution, we try to find an optimal solution by translating qubit recycling problem into an ILP model, and solve the model using the SCIP solver [Bolusani et al. 2024], a framework for Constraint Integer Programming. When the problem size is too large for SCIP to find optimal solutions in reasonable time, we estimate an upper-bound for the size of an optimal solution.

7.2.1 ILP Model. Recall that given a QDG in form of a $n \times n$ 0-1 matrix A, to find a maximal valid recycling strategy is to find a partial permutation matrix R (representing an injective partial map) such that AR is nilpotent, and the rank of R is maximized. This description can be roughly transformed into an ILP problem in Fig. 10. Here R consists of $n \times n$ 0-1 variables, and the constraints $\mathbf{1}^T \cdot R \leq \mathbf{1}$ and $R \cdot \mathbf{1} \leq \mathbf{1}$ is to guarantee that R is a partial permutation. The main difficulty is to translate "nilpotent" into a linear constraint.

$$\begin{aligned} \text{maximize} \quad & \mathbf{1}^T \cdot R \cdot \mathbf{1} \\ \text{subject to} \quad & AR \text{ nilpotent} \\ & \mathbf{1}^T \cdot R \leq \mathbf{1} \\ & R \cdot \mathbf{1} \leq \mathbf{1} \end{aligned}$$

Fig. 10. The ILP model.

We achieve this using the fact [Bang-Jensen and Gutin 2008] that: every acyclic graph has an acyclic ordering. That is, an ordering $p_1, ..., p_n$ such that for every $p_i \to p_j$, we have $i < j$. Since the nilpotent constraint is equivalent to requiring the digraph represented by AR is nilpotent, we introduce another n integer variables p_i representing the i-th qubit in an acyclic ordering, and the nilpotent constraint becomes: $\forall i, j.\ (AR)_{i,j} = 1 \implies p_i < p_j$, and additional constraints

$\forall i.\, 1 \le p_i \le n$ and $\forall i \ne j.\, p_i \ne p_j$. These constraints can be easily translated into $O(n^2)$ linear constraints at a cost of additional $O(n^2)$ variables.

The model then becomes:

$$\begin{array}{lll} \text{maximize} & \mathbf{1}^T \cdot R \cdot \mathbf{1} & \\ \text{subject to} & (AR)_{i,j} = 1 \implies p_i < p_j & \text{for any } i, j \\ & 1 \le p_i \le n & \text{for any } i \\ & p_i \ne p_j & \text{for any } i \ne j \\ & \mathbf{1}^T \cdot R \le \mathbf{1} & \\ & R \cdot \mathbf{1} \le \mathbf{1} & \end{array}$$

We introduce a boolean variable P_{ij} for those constraints $p_i \ne p_j$, where $P_{ij} = 1$ or 0 if and only if $p_i > p_j$ or $p_i < p_j$, respectively. The full model is:

$$\begin{array}{lll} \text{maximize} & \sum_{ij} R_{ij} & \\ \text{subject to} & p_i - p_j + n(AR)_{ij} \le n - 1 & \text{for any } i, j \\ & 1 \le p_i \le n & \text{for any } i \\ & 1 - n \le p_i - p_j - nP_{ij} \le -1 & \text{for any } i \ne j \\ & \sum_j R_{ij} \le 1 & \text{for any } j \\ & \sum_i R_{ij} \le 1 & \text{for any } i \\ \text{integers} & p_i & \text{for any } i \\ \text{binaries} & R_{ij}, P_{ij} & \text{for any } i, j \end{array}$$

Our model is more compact ($O(n^2)$ variables and constraints) compared with that of [DeCross et al. 2023] ($O(n^2)$ variables and $O(n^4)$ constraints), thus is potentially easier to solve.

7.2.2 Upper-Bound Estimator. If we are to have a size k solution for a QDG A, by Lm. 5.5, there must be a strictly upper-triangular submatrix B of order k. Therefore, there must be a row i_k with more than k 0s, and a column j_k with more than k 0s. Among the rest of rows and columns, there must be a row i_{k-1} with more than $k-1$ 0s, etc. Based on this idea, we have an upper-bound estimation for the size of the optimal solution. We count the number of 0s of each rows, and sort the counts in descending order obtaining $r_1, r_2, ..., r_n$. We do the same for the columns, and obtain $c_1, c_2, ..., c_n$. The upper bound is $\hat{k} = \min_{i=1,2,...,n}(\min(r_i, c_i) + 2(i-1))$.

7.3 Experimental Evaluation

This subsection presents experimental evaluation of the performance of Alg. 4 with 5 heuristics (namely, `Greedy`, `Max0s`, their look-ahead version `Greedy+LA` and `Max0s+LA`, and `Greedy+Max0s` that returns the better results from `Greedy` and `Max0s`), along with comparisons with recent related works. The following outlines the specific settings.

Metrics. We evaluated each method using metrics including the number of recycled qubits, result optimality and solving time, and the increase in circuit depth after recycling.

Dataset. We conducted evaluations using the 84 circuits from the RevLib [Wille et al. 2008] benchmark reported in [Paler et al. 2016]. Additionally, to facilitate comparisons with related works, we introduced a modified version of the dataset. In these modified circuits, each qubit is allocated before use and discarded at the end, effectively eliminating I/O qubits.

Comparative studies. We compare our algorithm with [Paler et al. 2016] and two recent related works [DeCross et al. 2023; Hua et al. 2023]. However, the latter two works do not explicitly support circuits with I/O qubits. In order to facilitate a fair comparison with them, on one hand, we

Circuit	W	#Recycled qubits (the more the better)						
		P	D	G	GL	M	ML	GM
pdc_307	619	464	505	505	505	508	508	508
spla_315	489	401	407	407	407	407	407	407
hwb9_304	170	81	121	121	119	119	119	121
ex5p_296	206	107	127	127	127	125	125	127
e64-bdd_295	195	114	126	126	126	126	126	126
hwb8_303	112	52	73	73	73	73	73	73
hwb7_302	73	31	45	45	45	44	44	45
hwb6_301	46	20	22	22	23	22	22	22

(a) For each circuit, we list its width in column "W", and the number of recycled qubits using various methods in sub-columns of "# Recycled qubits". Each sub-column corresponds to a method as follows: "P": those reported in [Paler et al. 2016]; "D": our implementation of [DeCross et al. 2023]'s algorithm; "G": `Greedy`; "M": `Max0s`; "GL": `Greedy+LA`; "ML": `Max0s+LA`; "GM": `Greedy+Max0s`. The best results among the methods are highlighted.

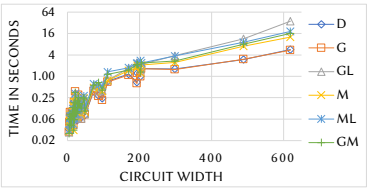

(b) Average time consumption.

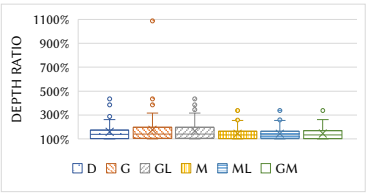

(c) Box plot of the ratios of circuit depths after and before recycling.

Fig. 11. Selected results of the evaluation on the RevLib benchmark.

additionally evaluate our algorithm on modified RevLib circuits, as described above; on the other hand, we implement the a version of the algorithm in [DeCross et al. 2023] that support I/O qubits.

Experimental setup. The experiments were conducted on a PC equipped with an AMD Ryzen 9 5950X CPU and 64GB of RAM, running Debian version 5.10.127-1.

7.3.1 Evaluation Results on RevLib. Selected results of the evaluation on the RevLib benchmark are shown in Fig. 11. Overall, all the methods achieves optimal on the majority of RevLib circuits; `Greedy+Max0s` achieves the highest number of best results.

Optimality. For 76 out of the 84 circuits, all of our methods, including our implementation of [DeCross et al. 2023]'s algorithm, achieved optimal results. In contrast, [Paler et al. 2016] achieved optimal results in only 59 of these circuits, and erroneously surpassed the optimal solution in 2 circuits. However, for the remaining 8 circuits, we could not determine if an optimal solution was obtained due to SCIP not terminating within 24 hours, and our estimated upper bounds did not match our solutions. The results for these 8 circuits are listed in Table 11a. For any pair of these methods, there exists a circuit where one method outperforms the other, except for [DeCross et al. 2023] and `Greedy`, which perform equally, and `Max0s` and `Max0s+LA`, which also perform equally. Furthermore, `Greedy+Max0s` achieves the highest number of optimal solutions, and performs equivalently or superiorly to [DeCross et al. 2023] and [Paler et al. 2016] in every example.

Time consumption. Fig. 11b shows the average time consumption (in logarithmic scale) of each method for RevLib circuits of different widths. The time consumption of [DeCross et al. 2023] and of `Greedy` are nearly the same and are the lowest among the methods. The `LA` methods incurs a significant overhead in time. Compared to [DeCross et al. 2023], the time consumption of `Greedy+Max0s` is approximately 1.5-3 times greater.

Increase in depth. Fig. 11c displays boxplots of the ratio between depth before and after recycling using each method. The performance of each method is comparable, with depth increase ranging

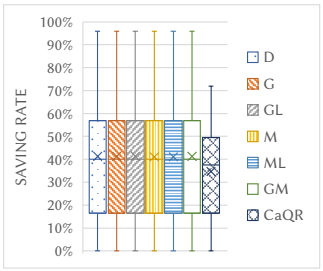

(a) Box plot of the rate of qubit saving across different methods.

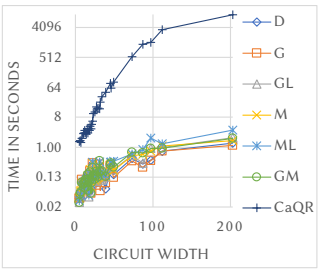

(b) Average time consumption.

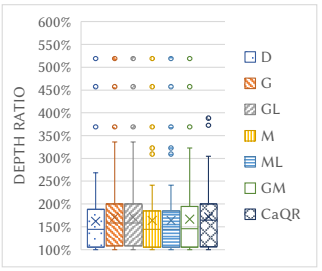

(c) Box plot of the ratios of circuit depths after and before recycling.

Fig. 12. Results of the evaluation on the modified RevLib benchmark.

from 144% to 176% on average. The ratios for methods `Max0s`, `Max0s+LA` and `Greedy+Max0s` have relatively consistent distribution.

7.3.2 Evaluation Results on Modified RevLib. Fig. 12 illustrates the evaluation results on the modified RevLib circuits, where we additionally assess CaQR[Hua et al. 2023]. We excluded 8 circuits where CaQR failed to terminate within 6 hours. The performance of all methods, except CaQR, closely mirrors the results from the unmodified RevLib circuits. Despite yielding a similar increase in circuit depth, CaQR exhibits significantly higher time consumption and noticeably lower qubit saving rates ($\frac{\#\text{Recycled qubits}}{\text{Circuit width}}$). The outliers in Fig. 12c, where CaQR demonstrates lower depth ratios, correspond to circuits where CaQR recycled considerably fewer qubits compared to other methods.

8 RELATED WORK

Width optimization for quantum circuits. Wire-recycling [Paler et al. 2016], CaQR [Hua et al. 2023], and two other recent works [DeCross et al. 2023; Sadeghi et al. 2022] investigate circuit width optimization in settings similar to ours, where opportunities for qubit reuse are created solely through topological deformations. Each algorithm in these works operates by reusing one qubit at a time and employs fundamentally similar criteria for 1-qubit reuse. Notably, [Sadeghi et al. 2022] and [DeCross et al. 2023], along with our `Greedy` heuristic, appear functionally similar, except that [Sadeghi et al. 2022] does not utilize the "dual-circuit" technique.

Among these works, [Sadeghi et al. 2022] and [DeCross et al. 2023] explicitly operate on a more compact causal cone abstraction (referred to as dependency lists in [Sadeghi et al. 2022]) rather than DAG representation. Our QDG effectively generalizes the causal cone by uniformly treating I/O qubits as special dependencies. Built on top of QDG, our triangularization formalization of the qubit recycling problem further provides criteria for valid recycling strategies, and enhances the intuitiveness of algorithm design, such as the `Greedy` heuristic and the "dual-circuit" technique. Our approach also naturally led to the design of `Max0s`, which outperforms [DeCross et al. 2023] on certain circuits.

CaQR [Hua et al. 2023] and [Sadeghi et al. 2022] additionally target SWAP reduction and improved fidelity or PST, which are critical aspects for NISQ applications. While these aspects are beyond the scope of this work, extending QDG with additional costs for each recycling strategy could potentially facilitate SWAP-aware qubit reuse. Furthermore, CaQR handles circuits where all gates commute, such as QAOA circuits, by reducing the problem to graph coloring. It is unclear to us how to generalize QDG to leverage non-trivial gate commutativity.

In addition to these works, REVS [Parent et al. 2015] and SQUARE [Ding et al. 2020] leverage uncomputation to create qubit-reuse opportunities, which also falls beyond the scope of our work.

Related problems in classical compiler optimizations. Two closely related problems in classical compiler optimizations are minimum register instruction sequencing (MRIS) [Govindarajan et al. 2003], and register saturation (RS) [Touati 2005]. MRIS appears fundamentally the same as qubit recycling. It asks to find a scheduling of instructions that requires minimum registers. However, the complexity of MRIS is not known. Opposite to qubit recycling, RS is an NP-hard problem that asks for the upper bound of needed registers in all possible scheduling. Another closely related problem is optimal code generation for DAGs, which is known to be NP-complete [Bruno and Sethi 1976]. Its objective is to minimize code length instead of the number of registers.

Related problem in the language of monoidal categories. In the context of monoidal categories, a closely related problem is computing the monoidal width [Lavore and Sobociński 2023]. Monoidal width quantifies the complexity of decomposing morphisms within monoidal categories, encompassing structural width measures for graphs like tree width and rank width. While monoidal width penalizes the composition operation along "large" objects and encourages the use of monoidal products, the qubit recycling problem seeks to minimize circuit width by penalizing the usage of monoidal products. For instance, the monoidal width of $f \otimes g$ is determined by $\max(w(f), w(g))$ using a weight function w, whereas a proper definition for circuit width should be in a form of $w(f) + w(g)$. Exploring the generalization of the qubit recycling problem to other settings presents an intriguing avenue for further investigation.

Compiler verification for quantum programs. There are numerous works on compiler verification and formulation of compiler correctness for various scenarios [Patterson and Ahmed 2019]. Few work targets the quantum settings. Amy et. al. [Amy et al. 2017] verified a compiler from Boolean expressions to reversible circuits in F*, with an aim to reduce circuit width. However, their verification uses a classical semantic model, where a state is of type $\mathbb{N} \to \mathbb{B}$. ReQWIRE [Rand et al. 2018], presents methods for verifying that ancillae are discarded in the desired state, and implements a verified compiler from classical functions to quantum oracles. Their semantics is parameterized with a context that maps variables to wire indices, serving a similar purpose as our *In*, *Out* lists. However, there is no notion for semantic preservation between quantum circuits in ReQWIRE, and it is not clear to us how their approach facilitates qubit recycling. VOQC [Hietala et al. 2021] and Giallar [Tao et al. 2022] aim to verify practical quantum circuit optimizers [Aleksandrowicz et al. 2019; Nam et al. 2018]. VOQC follows a CompCert-like approach that verifies each single optimization pass manually using sophisticated tactics; while Giallar seeks an almost automatic solution. As discussed previously, the verification techniques in these two works are not directly applicable to qubit recycling, where renaming and dynamic qubit allocation/discard are involved.

9 CONCLUSION AND FUTURE WORK

Qubit recycling involves finding a topologically identical quantum circuit that maximizes qubit reuse. By translating the problem to a matrix triangularization problem based on qubit dependency graphs, we demonstrated the NP-hardness of this problem. Additionally, we have developed a certified qubit recycler in Coq, This qubit recycler integrates validation and verification approaches. Byproducts of the certification include a verified implementation of Kahn's topological sort algorithm, and a mechanized proof of a version of the coherence theorem of symmetric monoidal categories. Our qubit recycler reaches optimal solutions for the majority circuits in the RevLib benchmark.

While our focus has been on topologically identical quantum circuits, where qubit reuse opportunities arise from disjoint instruction swaps, it is possible to further enhance qubit reuse

when a broader class of semantically equivalent quantum circuits is introduced. Potential future directions include extending the QDG-based approach by making use of a semantic domain with richer structures e.g., the ZX-calculus [Coecke and Kissinger 2017] and Quon [Liu et al. 2017], and fostering qubit reuse opportunities using additional circuit transformations guided by QDGs.

ACKNOWLEDGMENTS

We thank our anonymous referees for their suggestions and comments on earlier versions of this paper. We also thank Yuze Ruan and Yilong Wang for technical discussions. This work is partially supported by grants from National Natural Science Foundation of China under Grant No. 62202265, and from Beijing Natural Science Foundation under Grant No. Z220002.

DATA AVAILABILITY

An artifact containing our implementation, benchmarks and corresponding Coq proofs is publicly available on Zenodo [Jiang 2024].

REFERENCES

Samson Abramsky and Bob Coecke. 2004. A Categorical Semantics of Quantum Protocols. In *19th IEEE Symposium on Logic in Computer Science (LICS 2004), 14-17 July 2004, Turku, Finland, Proceedings*. IEEE Computer Society, 415–425. https://doi.org/10.1109/LICS.2004.1319636

Gadi Aleksandrowicz, Thomas Alexander, Panagiotis Barkoutsos, Luciano Bello, Yael Ben-Haim, David Bucher, Francisco Jose Cabrera-Hernández, Jorge Carballo-Franquis, Adrian Chen, Chun-Fu Chen, Jerry M. Chow, Antonio D. Córcoles-Gonzales, Abigail J. Cross, Andrew Cross, Juan Cruz-Benito, Chris Culver, Salvador De La Puente González, Enrique De La Torre, Delton Ding, Eugene Dumitrescu, Ivan Duran, Pieter Eendebak, Mark Everitt, Ismael Faro Sertage, Albert Frisch, Andreas Fuhrer, Jay Gambetta, Borja Godoy Gago, Juan Gomez-Mosquera, Donny Greenberg, Ikko Hamamura, Vojtech Havlicek, Joe Hellmers, Łukasz Herok, Hiroshi Horii, Shaohan Hu, Takashi Imamichi, Toshinari Itoko, Ali Javadi-Abhari, Naoki Kanazawa, Anton Karazeev, Kevin Krsulich, Peng Liu, Yang Luh, Yunho Maeng, Manoel Marques, Francisco Jose Martín-Fernández, Douglas T. McClure, David McKay, Srujan Meesala, Antonio Mezzacapo, Nikolaj Moll, Diego Moreda Rodríguez, Giacomo Nannicini, Paul Nation, Pauline Ollitrault, Lee James O'Riordan, Hanhee Paik, Jesús Pérez, Anna Phan, Marco Pistoia, Viktor Prutyanov, Max Reuter, Julia Rice, Abdón Rodríguez Davila, Raymond Harry Putra Rudy, Mingi Ryu, Ninad Sathaye, Chris Schnabel, Eddie Schoute, Kanav Setia, Yunong Shi, Adenilton Silva, Yukio Siraichi, Seyon Sivarajah, John A. Smolin, Mathias Soeken, Hitomi Takahashi, Ivano Tavernelli, Charles Taylor, Pete Taylour, Kenso Trabing, Matthew Treinish, Wes Turner, Desiree Vogt-Lee, Christophe Vuillot, Jonathan A. Wildstrom, Jessica Wilson, Erick Winston, Christopher Wood, Stephen Wood, Stefan Wörner, Ismail Yunus Akhalwaya, and Christa Zoufal. 2019. *Qiskit: An Open-source Framework for Quantum Computing*. https://doi.org/10.5281/zenodo.2562111

Matthew Amy, Martin Roetteler, and Krysta M. Svore. 2017. Verified Compilation of Space-Efficient Reversible Circuits. In *Computer Aided Verification - 29th International Conference, CAV 2017, Heidelberg, Germany, July 24-28, 2017, Proceedings, Part II (Lecture Notes in Computer Science, Vol. 10427)*, Rupak Majumdar and Viktor Kuncak (Eds.). Springer, 3–21. https://doi.org/10.1007/978-3-319-63390-9_1

Jrgen Bang-Jensen and Gregory Z. Gutin. 2008. *Digraphs: Theory, Algorithms and Applications*. https://doi.org/10.1007/978-1-84800-998-1

Suresh Bolusani, Mathieu Besançon, Ksenia Bestuzheva, Antonia Chmiela, João Dionísio, Tim Donkiewicz, Jasper van Doornmalen, Leon Eifler, Mohammed Ghannam, Ambros Gleixner, Christoph Graczyk, Katrin Halbig, Ivo Hedtke, Alexander Hoen, Christopher Hojny, Rolf van der Hulst, Dominik Kamp, Thorsten Koch, Kevin Kofler, Jurgen Lentz, Julian Manns, Gioni Mexi, Erik Mühmer, Marc E. Pfetsch, Franziska Schlösser, Felipe Serrano, Yuji Shinano, Mark Turner, Stefan Vigerske, Dieter Weninger, and Lixing Xu. 2024. *The SCIP Optimization Suite 9.0.* Technical Report. Optimization Online. https://optimization-online.org/2024/02/the-scip-optimization-suite-9-0/

Graham R. Brightwell and Peter Winkler. 1991. Counting Linear Extensions is #P-Complete. In *Proceedings of the 23rd Annual ACM Symposium on Theory of Computing, May 5-8, 1991, New Orleans, Louisiana, USA*, Cris Koutsougeras and Jeffrey Scott Vitter (Eds.). ACM, 175–181. https://doi.org/10.1145/103418.103441

John Bruno and Ravi Sethi. 1976. Code Generation for a One-Register Machine. *J. ACM* 23, 3 (jul 1976), 502–510. https://doi.org/10.1145/321958.321971

Bob Coecke and Aleks Kissinger. 2017. *Picturing Quantum Processes: A First Course in Quantum Theory and Diagrammatic Reasoning*. Cambridge University Press. https://doi.org/10.1017/9781316219317

Matthew DeCross, Eli Chertkov, Megan Kohagen, and Michael Foss-Feig. 2023. Qubit-Reuse Compilation with Mid-Circuit Measurement and Reset. *Phys. Rev. X* 13 (Dec 2023), 041057. Issue 4. https://doi.org/10.1103/PhysRevX.13.041057

Yongshan Ding, Xin-Chuan Wu, Adam Holmes, Ash Wiseth, Diana Franklin, Margaret Martonosi, and Frederic T. Chong. 2020. SQUARE: Strategic Quantum Ancilla Reuse for Modular Quantum Programs via Cost-Effective Uncomputation. In *2020 ACM/IEEE 47th Annual International Symposium on Computer Architecture (ISCA)*. 570–583. https://doi.org/10.1109/ISCA45697.2020.00054

Pavel Etingof, Shlomo Gelaki, Dmitri Nikshych, and Victor Ostrik. 2016. *Tensor categories*. American Mathematical Soc. https://bookstore.ams.org/surv-205

Guillaume Fertin, Irena Rusu, and Stéphane Vialette. 2015. Obtaining a Triangular Matrix by Independent Row-Column Permutations. In *Algorithms and Computation - 26th International Symposium, ISAAC 2015, Nagoya, Japan, December 9-11, 2015, Proceedings (Lecture Notes in Computer Science, Vol. 9472)*, Khaled M. Elbassioni and Kazuhisa Makino (Eds.). Springer, 165–175. https://doi.org/10.1007/978-3-662-48971-0_15

Austin G. Fowler, Matteo Mariantoni, John M. Martinis, and Andrew N. Cleland. 2012. Surface codes: Towards practical large-scale quantum computation. *Phys. Rev. A* 86 (Sep 2012), 032324. Issue 3. https://doi.org/10.1103/PhysRevA.86.032324

Ramaswamy Govindarajan, Hongbo Yang, José Nelson Amaral, Chihong Zhang, and Guang R. Gao. 2003. Minimum Register Instruction Sequencing to Reduce Register Spills in Out-of-Order Issue Superscalar Architectures. *IEEE Trans. Computers* 52, 1 (2003), 4–20. https://doi.org/10.1109/TC.2003.1159750

Ramsey W. Haddad. 1990. *Triangularization: a two-processor scheduling problem*. Ph. D. Dissertation. Stanford University, USA. https://searchworks.stanford.edu/view/507223

Chris Heunen and Jamie Vicary. 2019. *Categories for Quantum Theory: An Introduction*. Oxford University Press. https://doi.org/10.1093/oso/9780198739623.001.0001

Kesha Hietala, Robert Rand, Shih-Han Hung, Xiaodi Wu, and Michael Hicks. 2021. A Verified Optimizer for Quantum Circuits. *Proc. ACM Program. Lang.* 5, POPL, Article 37 (Jan 2021), 29 pages. https://doi.org/10.1145/3434318

Fei Hua, Yuwei Jin, Yan-Hao Chen, Suhas Vittal, Kevin Krsulich, Lev S. Bishop, John Lapeyre, Ali Javadi-Abhari, and Eddy Z. Zhang. 2023. CaQR: A Compiler-Assisted Approach for Qubit Reuse through Dynamic Circuit. In *Proceedings of the 28th ACM International Conference on Architectural Support for Programming Languages and Operating Systems, Volume 3, ASPLOS 2023, Vancouver, BC, Canada, March 25-29, 2023*, Tor M. Aamodt, Natalie D. Enright Jerger, and Michael M. Swift (Eds.). ACM, 59–71. https://doi.org/10.1145/3582016.3582030

Dominik Janzing, Pawel Wocjan, and Thomas Beth. 2003. Identity check is QMA-complete. https://doi.org/10.48550/ARXIV.QUANT-PH/0305050

Hanru Jiang. 2024. *PLDI2024 Artifact: Qubit Recycling Revisited*. https://doi.org/10.5281/zenodo.10721283

A. B. Kahn. 1962. Topological Sorting of Large Networks. *Commun. ACM* 5, 11 (nov 1962), 558–562. https://doi.org/10.1145/368996.369025

Aleks Kissinger and John van de Wetering. 2020. PyZX: Large Scale Automated Diagrammatic Reasoning. *Electronic Proceedings in Theoretical Computer Science* 318 (May 2020), 229–241. https://doi.org/10.4204/eptcs.318.14

Elena Di Lavore and Paweł Sobociński. 2023. Monoidal Width. arXiv:2212.13229 [cs.LO]

Xavier Leroy. 2009. Formal Verification of a Realistic Compiler. *Commun. ACM* 52, 7 (Jul 2009), 107–115. https://doi.org/10.1145/1538788.1538814

Zhengwei Liu, Alex Wozniakowski, and Arthur M. Jaffe. 2017. Quon 3D language for quantum information. *Proceedings of the National Academy of Sciences* 114, 10 (2017), 2497–2502. https://doi.org/10.1073/pnas.1621345114 arXiv:https://www.pnas.org/doi/pdf/10.1073/pnas.1621345114

Yunseong Nam, Neil J. Ross, Yuan Su, Andrew M. Childs, and Dmitri Maslov. 2018. Automated optimization of large quantum circuits with continuous parameters. *npj Quantum Information* 4, 1 (2018), 23. https://doi.org/10.1038/s41534-018-0072-4

Alexandru Paler, Robert Wille, and Simon J. Devitt. 2016. Wire recycling for quantum circuit optimization. *Phys. Rev. A* 94 (Oct 2016), 042337. Issue 4. https://doi.org/10.1103/PhysRevA.94.042337

Alex Parent, Martin Roetteler, and Krysta M. Svore. 2015. Reversible circuit compilation with space constraints. arXiv:1510.00377 [quant-ph]

Daniel Patterson and Amal Ahmed. 2019. The next 700 Compiler Correctness Theorems (Functional Pearl). *Proc. ACM Program. Lang.* 3, ICFP, Article 85 (Jul 2019), 29 pages. https://doi.org/10.1145/3341689

John Preskill. 2018. Quantum Computing in the NISQ era and beyond. *Quantum* 2 (Aug. 2018), 79. https://doi.org/10.22331/q-2018-08-06-79

Robert Rand, Jennifer Paykin, Dong-Ho Lee, and Steve Zdancewic. 2018. ReQWIRE: Reasoning about Reversible Quantum Circuits. In *Proceedings 15th International Conference on Quantum Physics and Logic, QPL 2018, Halifax, Canada, 3-7th June 2018 (EPTCS, Vol. 287)*, Peter Selinger and Giulio Chiribella (Eds.). 299–312. https://doi.org/10.4204/EPTCS.287.17

Silvain Rideau and Xavier Leroy. 2010. Validating Register Allocation and Spilling. In *Compiler Construction, 19th International Conference, CC 2010, Held as Part of the Joint European Conferences on Theory and Practice of Software, ETAPS 2010, Paphos, Cyprus, March 20-28, 2010. Proceedings (Lecture Notes in Computer Science, Vol. 6011)*, Rajiv Gupta (Ed.). Springer, 224–243.

https://doi.org/10.1007/978-3-642-11970-5_13

Movahhed Sadeghi, Soheil Khadirsharbiyani, and Mahmut Taylan Kandemir. 2022. Quantum Circuit Resizing. arXiv:2301.00720 [cs.ET]

Peter Selinger. 2004. Towards a Quantum Programming Language. *Mathematical. Structures in Comp. Sci.* 14, 4 (aug 2004), 527–586. https://doi.org/10.1017/S0960129504004256

Peter Selinger. 2005. Dagger Compact Closed Categories and Completely Positive Maps: (Extended Abstract). In *Proceedings of the 3rd International Workshop on Quantum Programming Languages, QPL 2005, DePaul University, Chicago, USA, June 30 - July 1, 2005 (Electronic Notes in Theoretical Computer Science, Vol. 170)*, Peter Selinger (Ed.). Elsevier, 139–163. https://doi.org/10.1016/j.entcs.2006.12.018

Runzhou Tao, Yunong Shi, Jianan Yao, Xupeng Li, Ali Javadi-Abhari, Andrew W. Cross, Frederic T. Chong, and Ronghui Gu. 2022. Giallar: push-button verification for the qiskit Quantum compiler. In *PLDI '22: 43rd ACM SIGPLAN International Conference on Programming Language Design and Implementation, San Diego, CA, USA, June 13 - 17, 2022*, Ranjit Jhala and Isil Dillig (Eds.). ACM, 641–656. https://doi.org/10.1145/3519939.3523431

Sid Ahmed Ali Touati. 2005. On the Optimality of Register Saturation. *Electron. Notes Theor. Comput. Sci.* 132, 1 (2005), 131–148. https://doi.org/10.1016/j.entcs.2005.01.033

John Wiegley. 2022. An axiom-free formalization of category theory in Coq. https://github.com/jwiegley/category-theory. Version 1.0.0.

H.S. Wilf. 1997. *On Crossing Numbers, and some Unsolved Problems.* Cambridge University Press, 557–562. https://doi.org/10.1017/CBO9780511662034.049

Robert Wille, Daniel Große, Lisa Teuber, Gerhard W. Dueck, and Rolf Drechsler. 2008. RevLib: An Online Resource for Reversible Functions and Reversible Circuits. In *38th IEEE International Symposium on Multiple-Valued Logic (ISMVL 2008), 22-23 May 2008, Dallas, Texas, USA*. IEEE Computer Society, 220–225. https://doi.org/10.1109/ISMVL.2008.43

A LEMMAS USED IN SEC. 4 AND 5

Lemma A.1. *For any simple circuits C and C' whose instructions are unique, C' is a topological sorting of C under $\prec_C$ if and only if $C' \sim C$.*

Proof. It suffices to prove that: for any adjacent instructions i and i' in a topological sorting C' of C under $\prec_C$,

$$i \mathbin{\#\#} i' \;\Leftrightarrow\; \neg((i \prec_C i') \vee (i' \prec_C i)). \tag{2}$$

Equation 2 is adequate because it is known that given topological sort C of a digraph D, another sequence C' is a topological sort of D if and only if C' can be obtained from C by swapping consecutive vertices that are not connected by an edge in D, and obviously C is a topological sorting of $D = (\{instr \in C\}, \prec_C)$.

We prove Equation 2 below.

- "$\Rightarrow$": By definition, $i \prec_C i'$ implies $args(i) \cap args(i') \neq \emptyset$, which contradicts with $i \mathbin{\#\#} i'$.
- "$\Leftarrow$": If $\neg(i \mathbin{\#\#} i')$, there is $q \in args(i) \cap args(i')$. Without loss of generality, assume $C' = C_1; i; i'; C_2$. Then we have $i \prec_C i'$ by definition, a contradiction.

□

Lemma A.2. *For any $G = (V, \rightarrow)$ such that $\forall v \in V.\, v \rightarrow v$, let $C = \textsc{ConstructCirc}(G)$, we have*

$$\forall v, v', \hat{v}.\; CX[v, \hat{v}] \prec_C CX[v', \hat{v}] \implies v \rightarrow v'.$$

Proof. Obvious by construction of C. □

Lemma A.3. *For any $G = (V, \rightarrow)$ such that $\forall v \in V.\, v \rightarrow v$, let $C = \textsc{ConstructCirc}(G)$, we have*

$$\forall v, v', \hat{v}, v''.\; CX[v, \hat{v}] \prec_C CX[v', \hat{v}](\prec_C)^+\mathbf{discard}[v''] \implies v' = v''.$$

Proof. Obvious by construction of C. □

Lemma A.4. *For any $G = (V, \rightarrow)$ where $v \rightarrow v$ for any $v \in V$, let $C = \textsc{ConstructCirc}(G)$, then $G = QDG(C)[V]$.*

Proof. By construction of C, for any $v \in V$, $\mathbf{alloc}[v]$ and $\mathbf{discard}[v]$ is in C. By definition of QDG, it suffices to show that

$$\forall v, v' \in V.\, v \rightarrow v' \Leftrightarrow \mathbf{alloc}[v](\prec_C)^+\mathbf{discard}[v'].$$

If $v = v'$, the result is obvious by construction of C. We consider the case when $v \neq v'$.

- "$\Rightarrow$": By construction of C, for each $v \rightarrow v'$ such that $v \neq v'$, there is $\hat{v}$ such that

  $$C = C_1; CX[v, \hat{v}]; C_2; CX[v', \hat{v}]; C_3,$$

  and $\hat{v}$ occur only in $CX[v, \hat{v}]$ and $CX[v', \hat{v}]$. Thus we have

  $$args(CX[v, \hat{v}]) \cap args(CX[v', \hat{v}]) \cap args(C_2) = \{\hat{v}\} \cap args(C_2) = \emptyset.$$

  By definition of $\prec_C$ and C is simple, we have

  $$\mathbf{alloc}[v](\prec_C)^+CX[v, \hat{v}] \prec_C CX[v', \hat{v}](\prec_C)^+\mathbf{discard}[v'].$$

  That is, $\mathbf{alloc}[v](\prec_C)^+\mathbf{discard}[v']$.

- "⇐": Given $\mathbf{alloc}[v](\prec_C)^+\mathbf{discard}[v']$ and $v \neq v'$, then by construction of C there is $\hat{v}$ such that $\mathbf{alloc}[v] \prec_C CX[v, \hat{v}]$ and
$$CX[v, \hat{v}](\prec_C)^+\mathbf{discard}[v'].$$
We prove by induction to show
$$\forall v \neq v', \hat{v}.\ CX[v, \hat{v}](\prec_C)^+\mathbf{discard}[v'] \implies v \to v'.$$
  - Base case: $CX[v, \hat{v}] \prec_C \mathbf{discard}[v']$.
Since $v \neq v'$ and $\hat{v} \neq v'$, $\neg(CX[v, \hat{v}] \prec_C \mathbf{discard}[v'])$. The goal vacuously holds.
  - Inductive step: $CX[v, \hat{v}] \prec_C i(\prec_C)^+\mathbf{discard}[v']$
We prove by case study on i. By definition of $\prec_C$ and construction of C, only the following two cases are possible.
    * $i = CX[v'', \hat{v}]$, $v'' \neq v$:
That is, $CX[v, \hat{v}] \prec_C CX[v'', \hat{v}] \prec_C{}^+ \mathbf{discard}[v']$. By Lemma A.2, $v \to v''$; by Lemma A.3, we have $v' = v''$. Thus $v \to v'$.
    * $i = CX[v, \hat{v}']$, $\hat{v}' \neq \hat{v}$:
We have $CX[v, \hat{v}'](\prec_C)^+\mathbf{discard}[v']$, by induction hypothesis we have $v \to v'$.

□

Lemma A.5. *A $(0,1)$-matrix A is nilpotent if and only if there exists a permutation matrix P such that P^TAP is strictly upper (or lower) triangular.*

Proof. Consider the corresponding digraph G of A.

$$\begin{aligned}
& A \text{ is nilpotent} \Leftrightarrow G \text{ is simple and acyclic} \\
\Leftrightarrow\ & \text{there is a permutation of vertices to obtain a topological sort of } G \\
\Leftrightarrow\ & \exists B, P.\ B = P^TAP \wedge \forall i \geq j.\ B_{ij} = 0 \ \Leftrightarrow\ \exists P.\ P^TAP \text{ is strict upper triangular.}
\end{aligned}$$

□

B PROOF OF LM 5.7

B.1 Notations and Preparation

We denote the set of $m \times n$ matrices over the field $\mathbb{F}_2$ of 2 elements (i.e., 0 and 1) by $M_{m,n}(\mathbb{F}_2)$, or $M_n(\mathbb{F}_2)$ for short when $m = n$. Throughout this section, P and Q denote the permutation matrices, P_σ denotes the permutation matrix corresponding to a permutation σ, e.g., $(k\ l)$ is the permutation that swaps k-th and l th elements, while $(k\ k)$ is identity; $\ulcorner$ and $\llcorner$ denote the upper and lower triangular matrices, respectively; $\mathbf{0}_{m\times n}$ and $\mathbf{1}_{m\times n}$ denote all 0s and all 1s matrices of size $m \times n$, respectively. Subscripts $m \times n$ are omitted when it is clear from the context.

For any $A, B \in M_{m,n}(\mathbb{F}_2)$, we use $A \sim B$ to denote the relation where B can be obtained by independently permuting rows and columns of A:

$$A \sim B \quad \text{iff} \quad (\exists P, Q.\, PAQ = B)\,.$$

It is straight forward to check that the following propositions hold.

Proposition B.1. *The relation $\sim$ is an equivalence relation.*

Proposition B.2. *For any $A, B \in M_{m,n}(\mathbb{F}_2)$ and permutations P, Q, $A \sim B \Leftrightarrow PAQ \sim PBQ$.*

Proposition B.3. $\ulcorner \sim \llcorner = \begin{bmatrix} & & 1 \\ & \iddots & \\ 1 & & \end{bmatrix} \ulcorner \begin{bmatrix} & & 1 \\ & \iddots & \\ 1 & & \end{bmatrix}$.

The next proposition shows that $\sim$ is preserved by padding constant columns or rows.

Proposition B.4. *For any $k \in \mathbb{N}$, $b \in \mathbb{F}_2$, and $A, B \in M_{m,n}(\mathbb{F}_2)$,*

$$[\, b\mathbf{1}_{m\times k}\ A\,] \sim [\, b\mathbf{1}_{m\times k}\ B\,] \Leftrightarrow A \sim B \Leftrightarrow \begin{bmatrix} b\mathbf{1}_{k\times n} \\ A \end{bmatrix} \sim \begin{bmatrix} b\mathbf{1}_{k\times n} \\ B \end{bmatrix}.$$

Proof. The second $\Leftrightarrow$ is derived from the first by taking transposes.

We prove $[\, b\mathbf{1}_{m\times k}\ A\,] \sim [\, b\mathbf{1}_{m\times k}\ B\,] \Leftrightarrow A \sim B$ by induction on k. The base case is trivial. The inductive case reduces to prove $[\, b\mathbf{1}_{m\times 1}\ A\,] \sim [\, b\mathbf{1}_{m\times 1}\ B\,] \Leftrightarrow A \sim B$ by induction hypothesis.

"$\Rightarrow$": By assumption, $\exists P, Q.\, P\,[\, b\mathbf{1}_{m\times 1}\ A\,]\, Q = [\, b\mathbf{1}_{m\times 1}\ PA\,]\, Q = [\, b\mathbf{1}_{m\times 1}\ B\,]$. Suppose $Q = P_\sigma$ for some σ, then the column $\sigma(1)$ of $[\, b\mathbf{1}_{m\times 1}\ B\,]$ is equal to $b\mathbf{1}_{m\times 1}$, its first row. Thus $[\, b\mathbf{1}_{m\times 1}\ B\,] = [\, b\mathbf{1}_{m\times 1}\ B\,]\, P_{(1\ \sigma(1))} = [\, b\mathbf{1}_{m\times 1}\ PA\,]\, P_\sigma P_{(1\ \sigma(1))} = [\, b\mathbf{1}_{m\times 1}\ PAP_{\sigma'}\,]$, for some σ'.

"$\Leftarrow$": By assumption, $\exists P, Q.\, B = PAQ$. Thus $P\,[\, b\mathbf{1}_{m\times 1}\ A\,] \begin{bmatrix} I \\ Q \end{bmatrix} = [\, bP\mathbf{1}_{m\times 1} IPAQ\,] = [\, b\mathbf{1}_{m\times 1}\ B\,]$. □

B.2 The Proof

With these notations, Lm 5.7 states that for any instance $A \in M_n(\mathbb{F}_2)$ of Wilf's question, we can find an instance $(\hat{A}, k) \in M_{n'}(\mathbb{F}_2) \times \mathbb{N}$ of the triangularization problem in Poly(n) time, such that

$$A \sim \ulcorner \iff \hat{A} \sim \begin{bmatrix} * & \left[\begin{smallmatrix} \mathbf{0} & 0 \\ \llcorner & \mathbf{0} \end{smallmatrix}\right]_{k\times k} \\ * & * \end{bmatrix}.$$

Proof. Given $A \in M_n(\mathbb{F}_2)$, let $k = n + 1$, and construct $\hat{A}$ blow:

$$\hat{A} ::= \begin{bmatrix} \mathbf{1}_{(n+1)\times(n+1)} & \left[\begin{smallmatrix} \mathbf{0} & 0 \\ A & \mathbf{0} \end{smallmatrix}\right] \\ \mathbf{1}_{(n+1)\times(n+1)} & \mathbf{1}_{(n+1)\times(n+1)} \end{bmatrix} \in M_{2(n+1)}(\mathbb{F}_2)$$

It is evident that the diagonal elements of $\hat{A}$ are 1s, making $(\hat{A}, k)$ a valid instance for the triangularization problem. It is also evident that the construction is of polynomial time.

To complete the proof, it suffices to show that

$$A \sim \ulcorner \overset{(1)}{\iff} \left[\begin{smallmatrix} \mathbf{0} & 0 \\ A & \mathbf{0}^T \end{smallmatrix}\right] \sim \left[\begin{smallmatrix} \mathbf{0} & 0 \\ \llcorner & \mathbf{0}^T \end{smallmatrix}\right] \overset{(2)}{\iff} \hat{A} \sim \begin{bmatrix} \mathbf{1} & \left[\begin{smallmatrix} \mathbf{0} & 0 \\ \llcorner_{n\times n} & \mathbf{0}^T \end{smallmatrix}\right] \\ \mathbf{1} & \mathbf{1} \end{bmatrix} \overset{(3)}{\iff} \hat{A} \sim \begin{bmatrix} * & \left[\begin{smallmatrix} \mathbf{0} & 0 \\ \llcorner_{n\times n} & \mathbf{0}^T \end{smallmatrix}\right] \\ * & * \end{bmatrix}.$$

Here (1), (2) follows from Prop. B.1-B.4; (3) is evident by counting constant columns/rows. □